

1
2
3
4
5
6
7
8
9
10
11
12
13
14
15
16
17
18
19
20
21
22
23
24
25
26
27
28
29
30
31
32
33
34
35
36
37
38
39
40
41

SARS-CoV-2 B.1.1.7 sensitivity to mRNA vaccine-elicited, convalescent and monoclonal antibodies

Dami A. Collier^{1,2,3*}, Anna De Marco^{4*}, Isabella A.T.M. Ferreira^{*1,2}, Bo Meng^{1,2*}, Rawlings Datir ^{*1,2,3}, Alexandra C. Walls⁵, Steven A. Kemp S^{1,2,3}, Jessica Bassi⁴, Dora Pinto⁴, Chiara Silacci Fregni⁴, Siro Bianchi⁴, M. Alejandra Tortorici⁵, John Bowen⁵, Katja Culap⁴, Stefano Jaconi⁴, Elisabetta Cameroni⁴, Gyorgy Snell⁶, Matteo S. Pizzuto⁴, Alessandra Franzetti Pellanda⁷, Christian Garzoni⁷, Agostino Riva⁸, The CITIID-NIHR BioResource COVID-19 Collaboration⁹, Anne Elmer¹⁰, Nathalie Kingston¹¹, Barbara Graves ¹¹, Laura E McCoy³, Kenneth GC Smith ^{1,2}, John R. Bradley ^{2,11}, Nigel Temperton¹², Lourdes Ceron-Gutierrez L¹³, Gabriela Barcenás-Morales ^{13,14}, The COVID-19 Genomics UK (COG-UK) consortium¹⁵, William Harvey¹⁶, Herbert W. Virgin⁶, Antonio Lanzavecchia⁴, Luca Piccoli⁴, Rainer Doffinger¹³, Mark Wills², David Veessler⁵, Davide Corti^{4*}, Ravindra K. Gupta^{1,2, 17,18,19*}

¹Cambridge Institute of Therapeutic Immunology & Infectious Disease (CITIID), Cambridge, UK.
²Department of Medicine, University of Cambridge, Cambridge, UK.
³Division of Infection and Immunity, University College London, London, UK.
⁴Humabs Biomed SA, a subsidiary of Vir Biotechnology, 6500 Bellinzona, Switzerland.
⁵Department of Biochemistry, University of Washington, Seattle, WA 98195, USA
⁶Vir Biotechnology, San Francisco, CA 94158, USA.
⁷Clinic of Internal Medicine and Infectious Diseases, Clinica Luganese Moncucco, 6900 Lugano, Switzerland
⁸Division of Infectious Diseases, Luigi Sacco Hospital, University of Milan, Milan, Italy
⁹The CITIID-NIHR BioResource COVID-19 Collaboration, see appendix 1 for author list
¹⁰NIHR Cambridge Clinical Research Facility, Cambridge, UK.
¹¹NIHR Bioresource, Cambridge, UK
¹²University of Kent, Canterbury, UK
¹³Department of Clinical Biochemistry and Immunology, Addenbrookes Hospital, UK
¹⁴Laboratorio de Inmunología, S-Cuautitlán, UNAM, Mexico
¹⁵<https://www.cogconsortium.uk>. Full list of consortium names and affiliations are in Appendix 2.
¹⁶Institute of Biodiversity, University of Glasgow, Glasgow, UK
¹⁷University of KwaZulu Natal, Durban, South Africa
¹⁸Africa Health Research Institute, Durban, South Africa
¹⁹Department of Infectious Diseases, Cambridge University Hospitals NHS Trust, Cambridge UK.

*Equal contribution

Correspondence: dcorti@vir.bio, rkg20@cam.ac.uk

Key words: SARS-CoV-2; COVID-19; antibody, vaccine, neutralising antibodies; mutation; variant

42 **Abstract**

43 **Severe Acute Respiratory Syndrome Coronavirus-2 (SARS-CoV-2) transmission is**
44 **uncontrolled in many parts of the world, compounded in some areas by higher**
45 **transmission potential of the B.1.1.7 variant now seen in 50 countries. It is unclear whether**
46 **responses to SARS-CoV-2 vaccines based on the prototypic strain will be impacted by**
47 **mutations found in B.1.1.7. Here we assessed immune responses following vaccination**
48 **with mRNA-based vaccine BNT162b2. We measured neutralising antibody responses**
49 **following a single immunization using pseudoviruses expressing the wild-type Spike**
50 **protein or the 8 amino acid mutations found in the B.1.1.7 spike protein. The vaccine sera**
51 **exhibited a broad range of neutralising titres against the wild-type pseudoviruses that**
52 **were modestly reduced against B.1.1.7 variant. This reduction was also evident in sera**
53 **from some convalescent patients. Decreased B.1.1.7 neutralisation was also observed with**
54 **monoclonal antibodies targeting the N-terminal domain (9 out of 10), the Receptor**
55 **Binding Motif (RBM) (5 out of 31), but not in neutralising mAbs binding outside the RBM.**
56 **Introduction of the E484K mutation in a B.1.1.7 background to reflect newly emerging**
57 **viruses in the UK led to a more substantial loss of neutralising activity by vaccine-elicited**
58 **antibodies and mAbs (19 out of 31) over that conferred by the B.1.1.7 mutations alone.**
59 **E484K emergence on a B.1.1.7 background represents a threat to the vaccine BNT162b.**

60

61 **Introduction**

62 The outbreak of a pneumonia of unknown cause in Wuhan, China in December 2019,
63 culminated in a global pandemic due to a novel viral pathogen, now known to be SARS-CoV-
64 2¹. The unprecedented scientific response to this global challenge has led to the rapid
65 development of vaccines aimed at preventing SARS-COV-2 infection and transmission.
66 Continued viral evolution led to the emergence and selection of SARS-CoV-2 variants with
67 enhanced infectivity/transmissibility^{2,3 4,5} and ability to circumvent drug⁶ and immune
68 control^{7,8}.

69 SARS-CoV-2 vaccines have recently been licensed that target the spike (S) protein,
70 either using mRNA or adenovirus vector technology with protection rates ranging from 62 to
71 95%⁹⁻¹¹. The BNT162b2 vaccine encodes the full-length trimerised S protein of SARS CoV-2
72 and is formulated in lipid nanoparticles for delivery to cells¹². Other vaccines include the
73 Moderna mRNA-1273 vaccine, which is also a lipid nanoparticle formulated S glycoprotein¹³
74 and the Oxford-AstraZeneca ChAdOx1 nCoV-19 vaccine (AZD1222) which is a replication-
75 deficient chimpanzee adenoviral vector ChAdOx1, containing the S glycoprotein¹⁴. The
76 duration of immunity conferred by these vaccines is as yet unknown. These vaccines were
77 designed against the Wuhan-1 isolate discovered in 2019. Concerns have been raised as to
78 whether these vaccines will be effective against newly emergent SARS-CoV-2 variants, such

79 as B.1.1.7 (N501Y.V1), B.1.351 (N501Y.V2) and P1 (N501Y.V3) that originated in the UK,
80 South Africa, and Brazil and are now being detected all over the world¹⁵⁻¹⁷.

81 In clinical studies of the Pfizer-BioNTech BNT162b2 vaccine, high levels of protection
82 against infection and severe disease were observed after the second dose¹⁰. Neutralising
83 geometric mean titre (GMT) was below cut-off in most cases after prime dose, but as
84 anticipated, titres substantially increased after boost immunization¹⁸. In older adults mean GMT
85 was only 12 in a preliminary analysis of 12 participants¹⁹ and increased to 109 after the second
86 dose.

87 In this study, we assess antibody responses against the the B.1.1.7 variant after
88 vaccination with the first and second doses of BNT162b2, showing modest reduction in
89 neutralisation against pseudoviruses bearing B.1.1.7 Spike mutations (Δ H69/V70, Δ I144,
90 N501Y, A570D, P681H, T716I, S982A and D1118H). In addition, by using a panel of human
91 neutralising monoclonal antibodies (mAbs) we show that the B.1.1.7 variant can escape
92 neutralisation mediated by most NTD-specific antibodies tested and by a fraction of RBM-
93 specific antibodies. Finally, we show that the recent emergence and transmission of B.1.1.7
94 viruses bearing the Spike E484K mutation results in significant additional loss of neutralisation
95 by BNT162b2 mRNA-elicited antibodies, convalescent sera and mAbs.

96

97 **Results**

98 Thirty seven participants had received the first dose of BNT162b2 mRNA vaccine three
99 weeks prior to blood draw for serum and peripheral blood mononuclear cells (PBMC)
100 collection. Median age was 63.5 years (IQR 47-84) and 33% were female. Serum IgG titres to
101 Nucleocapsid (N) protein, S and the S receptor binding domain (RBD) were assayed by particle
102 based flow cytometry on a Luminex analyser (**Extended Data Fig. 1a**). These data showed S
103 and RBD antibody titres much higher than in healthy controls, but lower than in individuals
104 recovered from COVID-19 and titres observed in therapeutic convalescent plasma. The raised
105 N titres relative to control could be the result of non-specific cross reactivity that is increased
106 following vaccination. However, the antibody response was heterogeneous with almost 100-
107 fold variation in IgG titres to S and RBD across the vaccinated participants.

108 Using lentiviral pseudotyping we studied WT (wild type bearing D614G) and mutant
109 B.1.1.7 S proteins (**Fig. 1a**) on the surface of enveloped virions in order to measure
110 neutralisation activity of vaccine-elicited sera. This system has been shown to give results
111 correlating with replication competent authentic virus^{20,21}. Eight out of 37 participants exhibited

112 no appreciable neutralisation against the WT pseudotyped virus following the first dose of
113 vaccines. The vaccine sera exhibited a range of inhibitory dilutions giving 50% neutralisation
114 (ID50) (**Fig. 1c-d**). The GMT against wild type (WT) following the second dose of vaccine was
115 an order of magnitude higher than after the first dose (318 vs 77) (Fig 1c-f). There was
116 correlation between full length S IgG titres and serum neutralisation titres (**Extended Data Fig.**
117 **1b**). A broad range of T cell responses was measured by IFN gamma FluoroSpot against SARS-
118 CoV-2 peptides in vaccinees. These cellular responses did not correlate with IgG S antibody
119 titres (**Extended Data Fig. 1c-d**).

120 We then generated mutated pseudoviruses carrying S protein with mutations N501Y,
121 A570D and the H69/V70 deletion. We observed no reduction in the ability of sera from
122 vaccinees to inhibit either WT or mutant virus (**Extended Data Fig. 2a, b**). A panel of sera
123 from ten recovered individuals also neutralised both wild type and the mutated viruses similarly
124 (**Extended Data Fig. 2c**). We next completed the full set of eight mutations in the S protein
125 present in B.1.1.7 variant (**Fig. 1a**), Δ H69/V70, Δ 144, N501Y and A570D in the S₁ subunit
126 and P681H, T716I, S982A and D1118H in the S₂ subunit. All constructs also contained D614G.
127 We found that among 29 individuals with neutralisation activity against the WT three weeks
128 after receiving a single dose of the the BNT162b2 mRNA vaccine, 20 showed evidence of
129 reduction in efficacy of antibodies against the B.1.1.7 mutant (**Fig. 1b-c, Extended Data Fig.**
130 **3**). The mean fold change reduction in sensitivity to first dose vaccine sera of B.1.1.7 compared
131 to WT was approximately 3.2 (SD 5.7). The variation is likely due to the low neutralisation
132 titres following first dose. Following the second dose, GMT was markedly increased compared
133 with first dose titres, and the mean fold change had reduced to 1.9 (SD 0.9) (**Fig. 1d-e**). Amongst
134 sera from 27 recovered individuals, the GMT at 50% neutralisation was 1334 for WT,
135 significantly higher than post second dose vaccination (**Fig. 1f-g**). The fold change in ID50 for
136 neutralisation of B.1.1.7 versus wild type (D614G) was 4.5 (**Fig. 1f-g and Extended Data Fig.**
137 **4**).

138 **B.1.1.7 with spike E484K mutation and neutralization by vaccine and convalescent sera**

139 The E484K substitution (**Fig. 2a**) is antigenically important, and has been reported as an escape
140 mutation for several monoclonal antibodies including C121, C144, REGN10933 and Ly-
141 CoV555²². E484K is also known to be present in the B.1.351 (501Y.V2) and P.1 (501Y.V3)
142 lineages in combination with amino acid replacements at N501 and K417. As of 10th Feb 2021,
143 twenty three English and two Welsh B.1.1.7 sequences from viral isolates contained the E484K

144 substitution (**Fig. 2b**). The number of B.1.1.7 sequences has been increasing since the start of
145 December 2020 (**Fig. 2c**). Phylogenetic analysis suggests that there have been multiple
146 independent acquisitions, with one lineage appearing to expand over time, indicating active
147 transmission (**Fig. 2b**). This has resulted in Public Health England naming this as a variant of
148 concern (VOC 202102/02)²³, triggering enhanced public health measures. There are as yet no
149 phenotypic data on the sensitivity to neutralisation for this virus or its spike protein.

150 We therefore generated pseudoviruses bearing B.1.1.7 spike mutations with or without
151 additional E484K and tested these against sera obtained after first and second dose mRNA
152 vaccine as well as against convalescent sera. Following second dose, we observed a significant
153 loss of neutralising activity for the pseudovirus with B.1.1.7 spike mutations and E484K (Fig
154 3d-e). The mean fold change for the E484K B.1.1.7 Spike was 6.7 compared to 1.9 for B.1.1.7,
155 relative to WT (**Fig. 3a-c**). Similarly when we tested a panel of convalescent sera with a range
156 of neutralisation titres (Fig. 1f-g), we observed additional loss of activity against the mutant
157 B.1.1.7 spike with E484K, with fold change of 11.4 relative to WT (**Fig. 3f-g**).

158 **B.1.1.7 variant escape from NTD- and RBM-specific mAb-mediated neutralization.**

159 To investigate the role of the full set of mutations in NTD, RBD and S2 present in the B.1.1.7
160 variant, we tested 60 mAbs isolated from 15 individuals that recovered from SARS-CoV-2
161 infection in early 2020 with an *in-vitro* pseudotyped neutralization assay using VeroE6 target
162 cells expressing Transmembrane protease serine 2 (TMPRSS2, **Extended Data Table 1**). We
163 found that 20 out of 60 (33.3%) mAbs showed a greater than 2-fold loss of neutralising
164 activity of B.1.1.7 variant compared to WT SARS-CoV-2 (**Fig. 4a,b** and **Extended Data Fig.**
165 **5**). Remarkably, the B.1.1.7 mutant virus was found to fully escape neutralization by 8 out of
166 10 NTD-targeting mAbs (80%), and partial escape from an additional mAb (10%) (**Fig. 4c**).
167 We previously showed that the deletion of residue 144 abrogates binding by 4 out of 6 NTD-
168 specific mAbs tested, possibly accounting for viral neutralization escape by most NTD-
169 specific antibodies²⁴. Of the 31 RBM-targeting mAbs, 5 (16.1%) showed more than 100-fold
170 decrease in B.1.1.7 neutralization, and additional 6 mAbs (19.4%) had a partial 2-to-10-fold
171 reduction (**Fig. 4d**). Finally, all RBD-specific non-RBM-targeting mAbs tested fully retained
172 B.1.1.7 neutralising activity (**Fig. 4e**).

173 To address the role of B.1.1.7 N501Y mutation in the neutralization escape from RBM-
174 specific antibodies, we tested the binding of 50 RBD-specific mAbs to WT and N501Y mutant
175 RBD by biolayer interferometry (**Fig. 4f** and **Extended Data Fig. 6**). The 5 RBM-specific

176 mAbs that failed to neutralize B.1.1.7 variant (**Fig. 4d**) showed a complete loss of binding to
177 N501Y RBD mutant (**Fig. 4g-h**), demonstrating a role for this mutation as an escape
178 mechanism for certain RBM-targeting mAbs.

179 The decreased neutralising activity of the immune sera from vaccinees and
180 convalescent patients against B.1.1.7, but not against Δ 69/70-501Y-570D mutant (**Fig. 1** and
181 **Extended Data Fig. 2**), could be the result of a loss of neutralising activity of both RBD- and
182 NTD-targeting antibodies, and suggests that the key mutation is Δ 144. RBD antibodies against
183 N501Y could play a role in decreased neutralisation by sera, with the overall impact possibly
184 modulated by other mutations present in B.1.1.7, as well as the relative dominance of NTD
185 versus RBM antibodies in polyclonal sera.

186 To assess the effect of E484K on this panel of mAbs we generated a SARS-CoV-2
187 pseudotype carrying the K417N, E484K and N501Y mutations (TM). The inclusion of the
188 K417N substitution was prompted by the observation that substitutions at this position have
189 been found in 5 sequences from recent viral isolates within the B.1.1.7 lineage (K417 to N, E
190 or R). This is in keeping with convergent evolution of the virus towards an RBD with N501Y,
191 E484K and K417N/T as evidenced by B.1.351 and P.1 lineages (K417N or K417T,
192 respectively) causing great concern globally. It is therefore important to assess this combination
193 going forward.

194 Importantly, mutations at K417 are reported to escape neutralization from mAbs,
195 including the recently approved mAb LY-CoV016^{22,25}. Out of the 60 mAbs tested, 20 (33.3%)
196 showed >10 fold loss of neutralising activity of TM mutant compared to WT SARS-CoV-2
197 (**Fig. 4 a-b** and **Extended Data Fig. 5**), and of these 19 are RBM-specific mAbs. As above,
198 we addressed the role of E484K mutation in escape from RBM-specific antibodies, by testing
199 the binding of 50 RBD-specific mAbs to WT and E484K mutant RBD by biolayer
200 interferometry (**Fig. 4f** and **Extended Data Fig. 7**). Out of the 19 RBM-specific mAbs that
201 showed reduced or loss of neutralization of TM mutant (**Fig. 4d**), 16 showed a complete or
202 partial loss of binding to E484K RBD mutant (**Fig. 4g-h**), consistent with findings that E484K
203 is an important viral escape mutation^{26, 39, 27}. Three of these 16 mAbs also lost binding to an
204 RBD carrying N501Y, indicating that a fraction of RBM antibodies are sensitive to both
205 N501Y and E484K mutations. Similarly, 3 of the 19 mAbs that lost neutralization of TM
206 mutant (S2D8, S2H7 and S2X128) were previously shown to lose binding and neutralization
207 to the K417V mutant, and here shown to be sensitive to either N501Y or E484K mutations.

208

209 **SARS-CoV-2 B.1.1.7 binds human ACE2 with higher affinity than WT**

210 SARS-CoV-2 and SARS-CoV enter host cells through binding of the S glycoprotein to
211 angiotensin converting enzyme 2 (ACE2)^{1,28}. Previous studies showed that the binding affinity
212 of SARS-CoV for human ACE2 correlated with the rate of viral replication in distinct species,
213 transmissibility and disease severity²⁹⁻³¹. However, the picture is unclear for SARS-CoV-2. To
214 understand the potential contribution of receptor interaction to infectivity, we set out to
215 evaluate the influence of the B.1.1.7 RBD substitution N501Y on receptor engagement. We
216 used biolayer interferometry to study binding kinetics and affinity of the purified human ACE2
217 ectodomain (residues 1-615) to immobilized biotinylated SARS-CoV-2 B.1.1.7 or WT RBDs.
218 We found that ACE2 bound to the B.1.1.7 RBD with an affinity of 22 nM compared to 133
219 nM for the WT RBD (**Extended Data Fig. 8**), in agreement with our previous deep-mutational
220 scanning measurements using dimeric ACE2³². Although ACE2 bound with comparable on-
221 rates to both RBDs, the observed dissociation rate constant was slower for B.1.1.7 than for the
222 WT RBD (**Table 1**).

223

224 To understand the impact of TM mutations (K417N, E484K and N501Y), we evaluated binding
225 of ACE2 to the immobilized TM RBD using biolayer interferometry. We determined an ACE2
226 binding affinity of 64 nM for the TM RBD which is driven by a faster off-rate than observed
227 for the B.1.1.7 RBD but slower than for the WT RBD. Based on our previous deep-mutational
228 scanning measurements using dimeric ACE2, we propose that the K417N mutation is slightly
229 detrimental to ACE2 binding explaining the intermediate affinity determined for the TM RBD
230 compared to the B.1.1.7 and WT RBDs, likely as a result of disrupting the salt bridge formed
231 with ACE2 residue D30. Enhanced binding of the B.1.1.7 RBD to human ACE2 resulting from
232 the N501Y mutation might participate in the efficient ongoing transmission of this newly
233 emergent SARS-CoV-2 lineage, and possibly reduced opportunity for antibody binding.
234 Although the TM RBD mutations found in B.1.351 are known to participate in immune
235 evasion^{33,34}, the possible contribution to transmissibility of enhanced ACE2 binding relative to
236 WT remains to be determined for this lineage.

237 **Discussion**

238 Serum neutralising activity is a correlate of protection for other respiratory viruses, including
239 influenza³⁵ and respiratory syncytial virus where prophylaxis with monoclonal antibodies has
240 been used in at-risk groups^{36,37}. Neutralising antibody titres appeared to be highly correlated
241 with vaccine protection against SARS-CoV-2 rechallenge in non-human primates, and
242 importantly, there was no correlation between T cell responses (as measured by ELISpot) and
243 protection³⁸. Moreover, passive transfer of purified polyclonal IgGs from convalescent
244 macaques protected naïve macaques against subsequent SARS-CoV-2 challenge³⁹. Coupled
245 with multiple reports of re-infection, there has therefore been significant attention placed on
246 virus neutralisation.

247 This study reports on the neutralisation by sera collected after both the first and second
248 doses of the BNT162b2 vaccine. The participants of this study were older adults, in line with
249 the targeting of this age group in the initial rollout of the vaccination campaign in the UK.
250 Participants showed similar neutralising activity against wild type pseudovirus as in the phase
251 I/II study¹². This is relevant for the UK and other countries planning to extend the gap between
252 doses of mRNA and adenovirus based vaccines from 3 to 12 weeks, despite lack of data for this
253 schedule for mRNA vaccines in particular.

254 The three mutations in S1 (N501Y, A570D, Δ H69/V70) did not appear to impact
255 neutralisation in a pseudovirus assay, consistent with data on N501Y having little effect on
256 neutralisation by convalescent and post vaccination sera⁴⁰. However, we demonstrated that a
257 pseudovirus bearing S protein with the full set of mutations present in the B.1.1.7 variant (i.e.,
258 Δ H69/V70, Δ 144, N501Y, A570D, P681H, T716I, S982A, D1118H) did result in small
259 reduction in neutralisation by sera from vaccinees that was more marked following the first
260 dose than the second dose. This could be related to increased breadth/potency/concentration of
261 antibodies following the boost dose. A reduction in neutralization titres from mRNA-elicited
262 antibodies in volunteers who received two doses (using both mRNA-1273 and BNT162b2
263 vaccines) was also observed by Wang et al.⁴¹ using pseudoviruses carrying the N501Y
264 mutation. Other studies also reported small reduction of neutralization against the B.1.1.7
265 variant against sera from individuals vaccinated with two doses of BNT162b2⁴² and mRNA-
266 1273⁴³. Xie et al did not find an effect of N501Y alone in the context of BNT162b2 vaccine
267 sera⁴⁴.

268 The reduced neutralising activity observed with polyclonal antibodies elicited by
269 mRNA vaccines observed in this study is further supported by the loss of neutralising activity
270 observed with human mAbs directed to both RBD and, to a major extent, to NTD. In the study
271 by Wang et al., 6 out of 17 RDB-specific mAbs isolated from mRNA-1273 vaccinated individuals
272 showed more than 100-fold neutralisation loss against N501Y mutant, a finding that is
273 consistent with the loss of neutralisation by 5 out of 29 RBM-specific mAbs described in this
274 study. However, the contribution of N501Y to loss of neutralisation activity of polyclonal
275 vaccine and convalescent sera is less clear, and interactions with other mutations likely.

276 Multiple variants, including the 501Y.V2 and B.1.1.7 lineages, harbor multiple
277 mutations as well as deletions in NTD, most of which are located in a site of vulnerability that
278 is targeted by all known NTD-specific neutralising antibodies^{24,45}. The role of NTD-specific
279 neutralising antibodies might be under-estimated, in part by the use of neutralization assays
280 based on target cells over-expressing ACE2 receptor. NTD-specific mAbs were suggested to
281 interfere with viral entry based on other accessory receptors, such as DC-SIGN and L-SIGN⁴⁶,
282 and their neutralization potency was found to be dependent on different in vitro culture
283 conditions²⁴. The observation that 9 out of 10 NTD-specific neutralising antibodies failed to
284 show a complete or near-complete loss of neutralising activity against B.1.1.7 indicates that this
285 new variant may have evolved also to escape from this class of antibodies, that may have a yet
286 unrecognized role in protective immunity. Wibmer et al.³⁴ have also recently reported the loss
287 of neutralization of 501Y.V2 by the NTD-specific mAb 4A8, likely driven by the R246I
288 mutation. This result is in line with the lack of neutralization of B.1.1.7 by the 4A8 mAb
289 observed in this study, likely caused by Δ 144 due to loss of binding²⁴. Finally, the role of NTD
290 mutations (in particular, L18F, Δ 242-244 and R246I) was further supported by the marked loss
291 of neutralization observed by Wibmer et al.³⁴ against 501Y.V2 compared to the chimeric
292 pseudotyped viral particle carrying only the RBD mutations K417N, E484K and N501Y. Taken
293 together, the presence of multiple escape mutations in NTD is supportive of the hypothesis that
294 this region of the spike, in addition to RBM, is also under immune pressure.

295 Worryingly, we have shown that there are multiple B.1.1.7 sequences in the UK bearing
296 E484K with early evidence of transmission as well as independent acquisitions. We measured
297 further reduction neutralisation titers by vaccine sera when E484K was present alongside the
298 B.1.1.7 S mutations. Wu and co-authors⁴³ have also shown that variants carrying the E484K
299 mutation resulted in 3-to-6 fold reduction in neutralization by sera from mRNA-1273

300 vaccinated individuals. Consistently, in this study we found that approximately 50% of the
301 RBM mAbs tested lost neutralising activity against SARS-CoV-2 carrying E484K. E484K has
302 been shown to impact neutralisation by monoclonal antibodies or convalescent sera, especially
303 in combination with N501Y and K417N^{16,26,47-49}. Wang et al also showed reduced neutralisation
304 by mRNA vaccine sera against E484K bearing pseudovirus³⁴.

305 Evidence for the importance role of NTD deletions in combination with E484K in immune
306 escape is provided by Andreano *et al.*²⁷ who describe the emergence of Δ 140 in virus co-
307 incubated with potently neutralising convalescent plasma, causing a 4-fold reduction in
308 neutralization titre. This Δ 140 mutant subsequently acquired E484K which resulted in a further
309 4-fold drop in neutralization titre indicating a two residue change across NTD and RBD
310 represents an effective pathway of escape that can dramatically inhibit the polyclonal response.

311 Our study was limited by modest sample size. Although the spike pseudotyping system has
312 been shown to faithfully represent full length infectious virus, there may be determinants
313 outside the S that influence escape from antibody neutralization either directly or indirectly in
314 a live replication competent system. On the other hand live virus systems allow replication and
315 therefore mutations to occur, and rigorous sequencing at multiple steps is needed.

316 Vaccines are a key part of a long term strategy to bring SARS-CoV-2 transmission under
317 control. Our data suggest that vaccine escape to current Spike directed vaccines designed
318 against the Wuhan strain will be inevitable, particularly given that E484K is emerging
319 independently and recurrently on a B.1.1.7 (501Y.V1) background, and given the rapid global
320 spread of B.1.1.7. Other major variants with E484K such as 501Y.V2 and V3 are also spreading
321 regionally. This should be mitigated by designing next generation vaccines with mutated S
322 sequences and using alternative viral antigens.

323

324 **Acknowledgements**

325 We would like to thank Cambridge University Hospitals NHS Trust Occupational Health
326 Department. We would also like to thank the NIHR Cambridge Clinical Research Facility and
327 staff at CUH and. We would like to thank Eleanor Lim and Georgina Okecha. We thank Dr
328 James Voss for the kind gift of HeLa cells stably expressing ACE2. RKG is supported by a
329 Wellcome Trust Senior Fellowship in Clinical Science (WT108082AIA). LEM is supported by

330 a Medical Research Council Career Development Award (MR/R008698/1). SAK is supported
331 by the Bill and Melinda Gates Foundation via PANGEA grant: OPP1175094. DAC is supported
332 by a Wellcome Trust Clinical PhD Research Fellowship. KGCS is the recipient of a Wellcome
333 Investigator Award (200871/Z/16/Z). This research was supported by the National Institute for
334 Health Research (NIHR) Cambridge Biomedical Research Centre, the Cambridge Clinical
335 Trials Unit (CCTU), and the NIHR BioResource. This study was supported by the National
336 Institute of General Medical Sciences (R01GM120553 to D.V.), the National Institute of
337 Allergy and Infectious Diseases (DP1AI158186 and HHSN272201700059C to D.V.), a Pew
338 Biomedical Scholars Award (D.V.), an Investigators in the Pathogenesis of Infectious Disease
339 Awards from the Burroughs Wellcome Fund (D.V.) and Fast Grants (D.V.). The views
340 expressed are those of the authors and not necessarily those of the NIHR or the Department of
341 Health and Social Care. JAGB is supported by the Medical Research Council
342 (MC_UP_1201/16). IATM is funded by a SANTHE award.

343

344 **Author contributions**

345 Conceived study: D.C., RKG, DAC. Designed study and experiments: RKG, DAC, LEM, JB,
346 MW, JT, LCG, GBM, RD, BG, NK, AE, M.P., D.V., L.P., A.D.M, J.B., D.C. Performed
347 experiments: BM, DAC, RD, IATMF, ACW, LCG, GBM. Interpreted data: RKG, DAC, BM,
348 RD, IATMF, ACW, LEM, JB, KGCS, DV. ADM, JB and CSF carried out pseudovirus
349 neutralization assays. DP produced pseudoviruses. MSP, LP, DV and DC designed the
350 experiments. MAT, JB, NS and SJ expressed and purified the proteins. KC, SJ and EC
351 sequenced and expressed antibodies. EC and KC performed mutagenesis for mutant expression
352 plasmids. ACW and S.B. performed binding assays. AR, AFP and CG contributed to donor's
353 recruitment and sample collection related to mAbs isolation. HWV, GS, AL, DV, LP, DV and
354 DC analyzed the data and prepared the manuscript with input from all authors.

355

356 **Competing interests**

357 A.D.M., J.B., D.P., C.S.F., S.B., K.C., N.S., E.C., G.S., S.J., A.L., H.W.V., M.S.P., L.P. and
358 D.C. are employees of Vir Biotechnology and may hold shares in Vir Biotechnology. H.W.V.
359 is a founder of PierianDx and Casma Therapeutics. Neither company provided funding for this
360 work or is performing related work. D.V. is a consultant for Vir Biotechnology Inc. The Veesler
361 laboratory has received a sponsored research agreement from Vir Biotechnology Inc. The

362 remaining authors declare that the research was conducted in the absence of any commercial
363 or financial relationships that could be construed as a potential conflict of interest. RKG has
364 received consulting fees from UMOVIS Lab, Gilead and ViiV.

365

366 **MATERIALS AND METHODS**

367 *Participant recruitment and ethics*

368 Participants who had received the first dose of vaccine and individuals with COVID-19
369 (Coronavirus Disease-19) were consented into the COVID-19 cohort of the NIHR Bioresource.
370 The study was approved by the East of England – Cambridge Central Research Ethics
371 Committee (17/EE/0025).

372

373 *SARS-CoV-2 serology by multiplex particle-based flow cytometry (Luminex):*

374 Recombinant SARS-CoV-2 N, S and RBD were covalently coupled to distinct carboxylated
375 bead sets (Luminex; Netherlands) to form a 3-plex and analyzed as previously described (Xiong
376 et al. 2020). Specific binding was reported as mean fluorescence intensities (MFI). Linear
377 regression was used to explore the association between antibody response, T cell response and
378 serum neutralisation in Stata 13. The Pearson correlation coefficient was reported.

379

380 *Recombinant expression of SARS-CoV-2-specific mAbs.*

381 Human mAbs were isolated from plasma cells or memory B cells of SARS-CoV-2 immune
382 donors, as previously described⁵⁰⁻⁵². Recombinant antibodies were expressed in ExpiCHO cells
383 at 37°C and 8% CO₂. Cells were transfected using ExpiFectamine. Transfected cells were
384 supplemented 1 day after transfection with ExpiCHO Feed and ExpiFectamine CHO Enhancer.
385 Cell culture supernatant was collected eight days after transfection and filtered through a 0.2
386 µm filter. Recombinant antibodies were affinity purified on an ÄKTA xpress fast protein liquid
387 chromatography (FPLC) device using 5 mL HiTrapTM MabSelectTM Prisma columns followed
388 by buffer exchange to Histidine buffer (20 mM Histidine, 8% sucrose, pH 6) using HiPrep
389 26/10 desalting columns

390

391 *Generation of S mutants*

392 Amino acid substitutions were introduced into the D614G pCDNA_SARS-CoV-2_S plasmid
393 as previously described⁵³ using the QuikChange Lightning Site-Directed Mutagenesis kit,

394 following the manufacturer's instructions (Agilent Technologies, Inc., Santa Clara, CA).
395 Sequences were checked by Sanger sequencing.

396 Preparation of B.1.1.7 or TM SARS-CoV-2 S glycoprotein-encoding-plasmid used to produce
397 SARS-CoV-2-MLV based on overlap extension PCR. Briefly, a modification of the overlap
398 extension PCR protocol⁵⁴ was used to introduce the nine mutations of the B.1.1.7 lineage or
399 the three mutations in TM mutant in the SARS-CoV-2 S gene. In a first step, 9 DNA
400 fragments with overlap sequences were amplified by PCR from a plasmid (phCMV1,
401 Genlantis) encoding the full-length SARS-CoV-2 S gene (BetaCoV/Wuhan-Hu-1/2019,
402 accession number mn908947). The mutations (del-69/70, del-144, N501Y, A570D, D614G,
403 P681H, S982A, T716I and D1118H or K417N, E484K and N501Y) were introduced by
404 amplification with primers with similar T_m. Deletion of the C-terminal 21 amino acids was
405 introduced to increase surface expression of the recombinant S⁵⁵. Next, 3 contiguous
406 overlapping fragments were fused by a first overlap PCR (step 2) using the utmost external
407 primers of each set, resulting in 3 larger fragments with overlapping sequences. A final overlap
408 PCR (step 3) was performed on the 3 large fragments using the utmost external primers to
409 amplify the full-length S gene and the flanking sequences including the restriction
410 sites KpnI and NotI. This fragment was digested and cloned into the expression plasmid
411 phCMV1. For all PCR reactions the Q5 Hot Start High fidelity DNA polymerase was used
412 (New England Biolabs Inc.), according to the manufacturer's instructions and adapting the
413 elongation time to the size of the amplicon. After each PCR step the amplified regions were
414 separated on agarose gel and purified using Illustra GFX™ PCR DNA and Gel Band
415 Purification Kit (Merck KGaA).

416

417 *Pseudotype virus preparation*

418 Viral vectors were prepared by transfection of 293T cells by using Fugene HD transfection
419 reagent (Promega). 293T cells were transfected with a mixture of 11ul of Fugene HD, 1μg of
420 pCDNAΔ19spike-HA, 1ug of p8.91 HIV-1 gag-pol expression vector^{56,57}, and 1.5μg of
421 pCSFLW (expressing the firefly luciferase reporter gene with the HIV-1 packaging signal).
422 Viral supernatant was collected at 48 and 72h after transfection, filtered through 0.45um filter
423 and stored at -80°C. The 50% tissue culture infectious dose (TCID₅₀) of SARS-CoV-2
424 pseudovirus was determined using Steady-Glo Luciferase assay system (Promega).

425

426 *Serum/plasma pseudotype neutralization assay*

427 Spike pseudotype assays have been shown to have similar characteristics as neutralisation
428 testing using fully infectious wild type SARS-CoV-2²⁰. Virus neutralisation assays were
429 performed on 293T cell transiently transfected with ACE2 and TMPRSS2 using SARS-CoV-2
430 spike pseudotyped virus expressing luciferase⁵⁸. Pseudotyped virus was incubated with serial
431 dilution of heat inactivated human serum samples or sera from vaccinees in duplicate for 1h at
432 37°C. Virus and cell only controls were also included. Then, freshly trypsinized 293T
433 ACE2/TMPRSS2 expressing cells were added to each well. Following 48h incubation in a 5%
434 CO₂ environment at 37°C, luminescence was measured using the Steady-Glo or Bright-Glo
435 Luciferase assay system (Promega). Neutralization was calculated relative to virus only
436 controls. Dilution curves were presented as a mean neutralization with standard error of the
437 mean (SEM). ID₅₀ values were calculated in GraphPad Prism. The ID₅₀ within groups were
438 summarised as a geometric mean titre and statistical comparison between groups were made
439 with Wilcoxon ranked sign test. In addition, the impact of the mutations on the neutralising
440 effect of the sera were expressed as fold change (FC) of ID₅₀ of the wild-type compared to
441 mutant pseudotyped virus. Statistical difference in the mean FC between groups was
442 determined using a 2-tailed t-test.

443 *IFN γ FluoroSpot assays*

444 Frozen PBMCs were rapidly thawed, and the freezing medium was diluted into 10ml of
445 TexMACS media (Miltenyi Biotech), centrifuged and resuspended in 10ml of fresh media
446 with 10U/ml DNase (Benzonase, Merck-Millipore via Sigma-Aldrich), PBMCs were
447 incubated at 37°C for 1h, followed by centrifugation and resuspension in fresh media
448 supplemented with 5% Human AB serum (Sigma Aldrich) before being counted. PBMCs
449 were stained with 2ul of each antibody: anti-CD3-fluorescein isothiocyanate (FITC), clone
450 UCHT1; anti-CD4-phycoerythrin (PE), clone RPA-T4; anti-CD8a-peridinin-chlorophyll
451 protein - cyanine 5.5 (PerCP Cy5.5), clone RPA-8a (all BioLegend, London, UK),
452 LIVE/DEAD Fixable Far Red Dead Cell Stain Kit (Thermo Fisher Scientific). PBMC
453 phenotyping was performed on the BD Accuri C6 flow cytometer. Data were analysed with
454 FlowJo v10 (Becton Dickinson, Wokingham, UK). 1.5 to 2.5 x 10⁵ PBMCs were incubated
455 in pre-coated Fluorospot plates (Human IFN γ FLUOROSPOT (Mabtech AB, Nacka Strand,
456 Sweden)) in triplicate with peptide mixes specific for Spike, Nucleocapsid and Membrane
457 proteins of SARS-CoV-2 (final peptide concentration 1 μ g/ml/peptide, Miltenyi Biotech) and
458 an unstimulated and positive control mix (containing anti-CD3 (Mabtech AB),

459 Staphylococcus Enterotoxin B (SEB), Phytohaemagglutinin (PHA) (all Sigma Aldrich)) at
460 37°C in a humidified CO₂ atmosphere for 48 hours. The cells and medium were decanted
461 from the plate and the assay developed following the manufacturer's instructions. Developed
462 plates were read using an AID iSpot reader (Oxford Biosystems, Oxford, UK) and counted
463 using AID EliSpot v7 software (Autoimmun Diagnostika GmbH, Strasberg, Germany). All
464 data were then corrected for background cytokine production and expressed as spot forming
465 units (SFU)/Million PBMC or CD3 T cells. The association between spike Tcell response,
466 spike specific antibody response and serum neutralisation was determined using linear
467 regression and the Pearson correlation coefficient between these variables were determined
468 using Stata 13.

469

470 *Ab discovery and recombinant expression*

471 Human mAbs were isolated from plasma cells or memory B cells of SARS-CoV or SARS-
472 CoV-2 immune donors, as previously described^{48,56-58}. Recombinant antibodies were
473 expressed in ExpiCHO cells at 37°C and 8% CO₂. Cells were transfected using
474 ExpiFectamine. Transfected cells were supplemented 1 day after transfection with ExpiCHO
475 Feed and ExpiFectamine CHO Enhancer. Cell culture supernatant was collected eight days
476 after transfection and filtered through a 0.2 µm filter. Recombinant antibodies were affinity
477 purified on an ÄKTA xpress FPLC device using 5 mL HiTrap™ MabSelect™ Prisma
478 columns followed by buffer exchange to Histidine buffer (20 mM Histidine, 8% sucrose, pH
479 6) using HiPrep 26/10 desalting columns.

480

481 *MAbs pseudovirus neutralization assay*

482 MLV-based SARS-CoV-2 S-glycoprotein-pseudotyped viruses were prepared as previously
483 described (Pinto et al., 2020). HEK293T/17cells were cotransfected with a WT, B.1.1.7 or
484 TM SARS-CoV-2 spike glycoprotein-encoding-plasmid, an MLV Gag-Pol packaging
485 construct and the MLV transfer vector encoding a luciferase reporter using X-tremeGENE
486 HP transfection reagent (Roche) according to the manufacturer's instructions. Cells were
487 cultured for 72 h at 37°C with 5% CO₂ before harvesting the supernatant. VeroE6 stably
488 expressing human TMPRSS2 were cultured in Dulbecco's Modified Eagle's Medium
489 (DMEM) containing 10% fetal bovine serum (FBS), 1% penicillin–streptomycin (100 I.U.
490 penicillin/mL, 100 µg/mL), 8 µg/mL puromycin and plated into 96-well plates for 16–24 h.
491 Pseudovirus with serial dilution of mAbs was incubated for 1 h at 37°C and then added to the
492 wells after washing 2 times with DMEM. After 2–3 h DMEM containing 20% FBS and 2%

493 penicillin–streptomycin was added to the cells. Following 48-72 h of infection, Bio-Glo
494 (Promega) was added to the cells and incubated in the dark for 15 min before reading
495 luminescence with Synergy H1 microplate reader (BioTek). Measurements were done in
496 duplicate and relative luciferase units were converted to percent neutralization and plotted
497 with a non-linear regression model to determine IC50 values using GraphPad PRISM
498 software (version 9.0.0).

499
500 *Antibody binding measurements using bio-layer interferometry (BLI)*

501 MAbs were diluted to 3 µg/ml in kinetic buffer (PBS supplemented with 0.01% BSA) and
502 immobilized on Protein A Biosensors (FortéBio). Antibody-coated biosensors were incubated
503 for 3 min with a solution containing 5 µg/ml of WT, N501Y or E484K SARS-CoV-2 RBD in
504 kinetic buffer, followed by a 3-min dissociation step. Change in molecules bound to the
505 biosensors caused a shift in the interference pattern that was recorded in real time using an
506 Octet RED96 system (FortéBio). The binding response over time was used to calculate the
507 area under the curve (AUC) using GraphPad PRISM software (version 9.0.0).

508
509 *Production of SARS-CoV-2 and B.1.1.7 receptor binding domains and human ACE2*

510 The SARS-CoV-2 RBD (BEI NR-52422) construct was synthesized by GenScript into CMVR
511 with an N-terminal mu-phosphatase signal peptide and a C-terminal octa-histidine tag
512 (GHHHHHHHH) and an avi tag. The boundaries of the construct are N-₃₂₈RFPN₃₃₁ and
513 ₅₂₈KKST₅₃₁-C⁵⁹. The B.1.1.7 RBD gene was synthesized by GenScript into pCMVR with the
514 same boundaries and construct details with a mutation at N501Y. These plasmids were
515 transiently transfected into Expi293F cells using Expi293F expression medium (Life
516 Technologies) at 37°C 8% CO₂ rotating at 150 rpm. The cultures were transfected using PEI
517 cultivated for 5 days. Supernatants were clarified by centrifugation (10 min at 4000xg) prior to
518 loading onto a nickel-NTA column (GE). Purified protein was biotinylated overnight using
519 BirA (Biotin ligase) prior to size exclusion chromatography (SEC) into phosphate buffered
520 saline (PBS). Human ACE2-Fc (residues 1-615 with a C-terminal thrombin cleavage site and
521 human Fc tag) were synthesized by Twist. Clarified supernatants were affinity purified using
522 a Protein A column (GE LifeSciences) directly neutralized and buffer exchanged. The Fc tag
523 was removed by thrombin cleavage in a reaction mixture containing 3 mg of recombinant
524 ACE2-FC ectodomain and 10 µg of thrombin in 20 mM Tris-HCl pH8.0, 150 mM NaCl and
525 2.5 mM CaCl₂. The reaction mixture was incubated at 25°C overnight and re-loaded on a
526 Protein A column to remove uncleaved protein and the Fc tag. The cleaved protein was further

527 purified by gel filtration using a Superdex 200 column 10/300 GL (GE Life Sciences)
528 equilibrated in PBS.

529

530 *Protein affinity measurement using bio-layer interferometry*

531 Biotinylated RBD (WT, N501Y, or TM) were immobilized at 5 ng/uL in undiluted 10X
532 Kinetics Buffer (Pall) to SA sensors until a load level of 1.1nm. A dilution series of either
533 monomeric ACE2 or Fab in undiluted kinetics buffer starting at 1000-50nM was used for 300-
534 600 seconds to determine protein-protein affinity. The data were baseline subtracted and the
535 plots fitted using the Pall FortéBio/Sartorius analysis software (version 12.0). Data were plotted
536 in Prism.

537

538 Statistical analysis

539 Linear regression was used to explore the association between antibody response, T cell
540 response and serum neutralisation in Stata 13. The Pearson correlation coefficient was reported.

541

542 Neutralisation data analysis

543 Neutralization was calculated relative to virus only controls. Dilution curves were presented as
544 a mean neutralization with standard error of the mean (SEM). IC50 values were calculated in
545 GraphPad Prism. The inhibitory dilution (ID50) within groups were summarised as a geometric
546 mean titre and statistical comparison between groups were made with Wilcoxon ranked sign
547 test. In addition, the impact of the mutations on the neutralising effect of the sera were
548 expressed as fold change of ID50 of the wild-type compared to mutant pseudotyped virus.
549 Statistical difference in the mean FC between groups was determined using a 2-tailed t-test

550

551

552 IFN γ FluoroSpot assay data analysis

553 The association between spike Tcell response, spike specific antibody response and serum
554 neutralisation was determined using linear regression and the Pearson correlation coefficient
555 between these variables were determined using Stata 13.

556

557 *Data availability.*

558 The neutralization and BLI data shown in Fig. 4 and Extended Data Fig. 5-7 can be found in
559 **Source Data Fig. 4**. Other data are available from the corresponding author on request.

560

561

562

563

564 **Table 1. Kinetic analysis of human ACE2 binding to SARS-CoV-2 Wuhan-1, N501Y and**
565 **N501Y/ E484K/ K417N (TM) RBDs by biolayer interferometry.** Values reported represent
566 the global fit to the data shown in Extended Data Fig. 8.

567

		SARS-CoV-2 RBD WT	SARS-CoV-2 RBD N501Y	SARS-CoV-2 RBD TM
K_D (nM)		133	22	64
k_{on} (M⁻¹.s⁻¹)	hACE2	1.3*10 ⁵	1.4*10 ⁵	1.3*10 ⁵
k_{off} (s⁻¹)		1.8*10 ⁻²	3*10 ⁻³	8.5*10 ⁻³

568

569

570

Extended Data Table 1. Neutralization, V gene usage and other properties of tested mAbs.

mAb	Domain (site)	VH usage (% id.)	Source (DSO)	IC50 WT (ng/ml)	IC50 B.1.1.7 (ng/ml)	ACE2 blocking	SARS-CoV	Escape residues	Ref.
4A8	NTD (i)	1-24	N/A	38	-	Neg.	-	S12P; C136Y; Y144del; H146Y; K147T; R246A	⁶⁰
S2L26	NTD (i)	1-24 (97.2)	Hosp. (52)	70	-	Neg.	-	N/A	²⁴
S2L50	NTD (i)	4-59 (95.4)	Hosp. (52)	264	50	Neg.	-	N/A	²⁴
S2M28	NTD (i)	3-33 (97.6)	Hosp. (46)	295	12'207	Neg.	-	P9S/Q; S12P; C15F/R; L18P; Y28C; A123T; C136Y; G142D; Y144del; K147Q/T; R246G; P251L; G252C	²⁴
S2X107	NTD (i)	4-38-2 (97)	Sympt. (75)	388	-	Neg.	-	N/A	²⁴
S2X124	NTD (i)	3-30 (99)	Sympt. (75)	221	-	Neg.	-	N/A	²⁴
S2X158	NTD (i)	1-24 (96.3)	Sympt. (75)	56	-	Neg.	-	N/A	²⁴
S2X28	NTD (i)	3-30 (97.9)	Sympt. (48)	1'399	-	Neg.	-	P9S; S12P; C15W; L18P; C136G/Y; F140S; L141S; G142C/D; Y144C/N; K147T/Q/E; R158G; L244S; R246G	²⁴
S2X303	NTD (i)	2-5 (95.9)	Sympt. (125)	69	-	Neg.	-	N/A	²⁴
S2X333	NTD (i)	3-33 (96.5)	Sympt. (125)	66	-	Neg.	-	P9L; S12P; C15S/Y; L18P; C136G/Y; F140C; G142D; K147T	²⁴
S2D106	RBD (I/RBM)	1-69 (97.2)	Hosp. (98)	27	20	Strong	-	N/A	⁸
S2D19	RBD (I/RBM)	4-31 (99.7)	Hosp. (49)	128	75'200	Moderate	-	N/A	⁸
S2D32	RBD (I/RBM)	3-49 (98.3)	Hosp. (49)	26	11	Strong	-	N/A	⁸
S2D65	RBD (I/RBM)	3-9 (96.9)	Hosp. (49)	24	12	Weak	-	N/A	⁸
S2D8	RBD (I/RBM)	3-23 (96.5)	Hosp. (49)	27	58'644	Strong	-	N/A	⁸
S2D97	RBD (I/RBM)	2-5 (96.9)	Hosp. (98)	20	17	Weak	-	N/A	⁸
S2E11	RBD (I/RBM)	4-61 (98.3)	Hosp. (51)	27	16	Weak	-	N/A	⁸
S2E12	RBD (I/RBM)	1-58 (97.6)	Hosp. (51)	27	31	Strong	-	G476S (3x)	^{8,61}
S2E13	RBD (I/RBM)	1-18 (96.2)	Hosp. (51)	34	77	Strong	-	N/A	⁸
S2E16	RBD (I/RBM)	3-30 (98.3)	Hosp. (51)	36	38	Strong	-	N/A	⁸
S2E23	RBD (I/RBM)	3-64 (96.9)	Hosp. (51)	139	180	Strong	-	N/A	⁸
S2H14	RBD (I/RBM)	3-15 (100)	Sympt. (17)	460	64'463	Weak	-	N/A	^{8,62}
S2H19	RBD (I/RBM)	3-15 (98.6)	Sympt. (45)	239	-	Weak	-	N/A	⁸
S2H58	RBD (I/RBM)	1-2 (97.9)	Sympt. (45)	27	14	Strong	-	N/A	⁸
S2H7	RBD (I/RBM)	3-66 (98.3)	Sympt. (17)	492	573	Weak	-	N/A	⁸
S2H70	RBD (I/RBM)	1-2 (99)	Sympt. (45)	147	65	Weak	-	N/A	⁸
S2H71	RBD (I/RBM)	2-5 (99)	Sympt. (45)	36	9	Moderate	-	N/A	⁸
S2M11	RBD (I/RBM)	1-2 (96.5)	Hosp. (46)	11	4	Weak	-	Y449N; L455F; E484K; E484Q; F490L; F490S; S494P	^{8,61}

S2N12	RBD (I/RBM)	4-39 (97.6)	Hosp. (51)	76	40	Strong	-	N/A	⁸
S2N22	RBD (I/RBM)	3-23 (96.5)	Hosp. (51)	32	21	Strong	-	N/A	⁸
S2N28	RBD (I/RBM)	3-30 (97.2)	Hosp. (51)	72	21	Strong	-	N/A	⁸
S2X128	RBD (I/RBM)	1-69-2 (97.6)	Sympt. (75)	50	112	Strong	-	N/A	⁸
S2X16	RBD (I/RBM)	1-69 (97.6)	Sympt. (48)	45	103	Strong	-	N/A	⁸
S2X192	RBD (I/RBM)	1-69 (96.9)	Sympt. (75)	326	-	Weak	-	N/A	⁸
S2X227	RBD (I/RBM)	1-46 (97.9)	Sympt. (75)	26	14	Strong	-	N/A	
S2X246	RBD (I/RBM)	3-48 (96.2)	Sympt. (75)	35	30	Strong	-	N/A	
S2X30	RBD (I/RBM)	1-69 (97.9)	Sympt. (48)	32	53	Strong	-	N/A	⁸
S2X324	RBD (I/RBM)	2-5 (97.3)	Sympt. (125)	8	23	Strong	-	N/A	
S2X58	RBD (I/RBM)	1-46 (99)	Sympt. (48)	32	47	Strong	-	N/A	⁸
S2H90	RBD (II)	4-61 (96.6)	Sympt. (81)	77	32	Strong	+	N/A	⁸
S2H94	RBD (II)	3-23 (93.4)	Sympt. (81)	123	144	Strong	+	N/A	⁸
S2H97	RBD (V)	5-51 (98.3)	Sympt. (81)	513	248	Weak	+	N/A	
S2K15	RBD (II)	2-26 (99.3)	Sympt. (87)	361	235	0	+	N/A	
S2K21	RBD (II)	3-33 (96.2)	Sympt. (118)	201	189	0	+	N/A	
S2K30	RBD (II)	1-2 (97.2)	Sympt. (87)	185	134	0	+	N/A	
S2K63v2	RBD (II)	3-30-3 (95.6)	Sympt. (118)	144	215	0	+	N/A	
S2L17	RBD (?)	5-10-1 (98.3)	Hosp. (51)	313	127	Moderate	+	N/A	⁸
S2L49	RBD (?)	3-30 (97.9)	Hosp. (51)	24	32	Neg.	+	N/A	⁸
S2X259	RBD (IIa)	1-69 (94.1)	Sympt. (75)	145	91	Moderate	+	N/A	
S2X305	RBD (?)	1-2 (95.1)	Sympt. (125)	34	21	Strong	-	N/A	
S2X35	RBD (IIa)	1-18 (98.6)	Sympt. (48)	140	143	Strong	+	N/A	⁶²
S2X450	RBD (?)	2-26 (96.9)	Sympt. (271)	368	198	Strong	+	N/A	
S2X475	RBD (?)	3-21 (93.8)	Sympt. (271)	1'431	851	Strong	+	N/A	
S2X607	RBD (?)	3-66 (95.4)	Sympt. (271)	41	23	Strong	-	N/A	
S2X608	RBD (?)	1-33 (93.2)	Sympt. (271)	21	35	Strong	-	N/A	
S2X609	RBD (?)	1-69 (93.8)	Sympt. (271)	47	35	Strong	-	N/A	
S2X613	RBD (I)	1-2 (91.7)	Sympt. (271)	28	19	Strong	-	N/A	
S2X615	RBD (I)	3-11 (94.8)	Sympt. (271)	23	17	Strong	-	N/A	
S2X619	RBD (?)	1-69 (92.7)	Sympt. (271)	36	60	Strong	-	N/A	
S2X620	RBD (?)	3-53 (95.1)	Sympt. (271)	34	45	Strong	-	N/A	

id., identity. DSO, days after symptom onset. * as described in Piccoli et al and McCallum et al. N/A, not available; -, not neutralising

571

572

573

574 **References**

575

- 576 1 Zhou, P. *et al.* A pneumonia outbreak associated with a new coronavirus of probable
577 bat origin. *Nature* **579**, 270-273, doi:10.1038/s41586-020-2012-7 (2020).
- 578 2 Davies, N. G. *et al.* Estimated transmissibility and severity of novel SARS-CoV-2
579 Variant of Concern 202012/01 in England. *medRxiv*, 2020.2012.2024.20248822,
580 doi:10.1101/2020.12.24.20248822 (2020).
- 581 3 Volz, E. *et al.* Transmission of SARS-CoV-2 Lineage B.1.1.7 in England: Insights from
582 linking epidemiological and genetic data. *medRxiv*, 2020.2012.2030.20249034,
583 doi:10.1101/2020.12.30.20249034 (2021).
- 584 4 Korber, B. *et al.* Tracking Changes in SARS-CoV-2 Spike: Evidence that D614G
585 Increases Infectivity of the COVID-19 Virus. *Cell* **182**, 812-827 e819,
586 doi:10.1016/j.cell.2020.06.043 (2020).
- 587 5 Yurkovetskiy, L. *et al.* Structural and Functional Analysis of the D614G SARS-CoV-2
588 Spike Protein Variant. *Cell* **183**, 739-751 e738, doi:10.1016/j.cell.2020.09.032 (2020).
- 589 6 Martinot, M. *et al.* Remdesivir failure with SARS-CoV-2 RNA-dependent RNA-
590 polymerase mutation in a B-cell immunodeficient patient with protracted Covid-19.
591 *Clin Infect Dis*, doi:10.1093/cid/ciaa1474 (2020).
- 592 7 Kemp, S. *et al.* Neutralising antibodies in Spike mediated SARS-CoV-2 adaptation.
593 *medRxiv*, 2020.2012.2005.20241927, doi:10.1101/2020.12.05.20241927 (2020).
- 594 8 Thomson, E. C. *et al.* The circulating SARS-CoV-2 spike variant N439K maintains
595 fitness while evading antibody-mediated immunity. *bioRxiv*, 1-49,
596 doi:papers3://publication/doi/10.1101/2020.11.04.355842 (2020).
- 597 9 Baden, L. R. *et al.* Efficacy and Safety of the mRNA-1273 SARS-CoV-2 Vaccine. *N Engl*
598 *J Med*, doi:10.1056/NEJMoa2035389 (2020).
- 599 10 Polack, F. P. *et al.* Safety and Efficacy of the BNT162b2 mRNA Covid-19 Vaccine. *N*
600 *Engl J Med* **383**, 2603-2615, doi:10.1056/NEJMoa2034577 (2020).
- 601 11 Voysey, M. *et al.* Safety and efficacy of the ChAdOx1 nCoV-19 vaccine (AZD1222)
602 against SARS-CoV-2: an interim analysis of four randomised controlled trials in Brazil,
603 South Africa, and the UK. *Lancet* **397**, 99-111, doi:10.1016/S0140-6736(20)32661-1
604 (2021).
- 605 12 Mulligan, M. J. *et al.* Phase I/II study of COVID-19 RNA vaccine BNT162b1 in adults.
606 *Nature* **586**, 589-593, doi:10.1038/s41586-020-2639-4 (2020).
- 607 13 Corbett, K. S. *et al.* SARS-CoV-2 mRNA Vaccine Development Enabled by Prototype
608 Pathogen Preparedness. *bioRxiv*, 2020.2006.2011.145920,
609 doi:10.1101/2020.06.11.145920 (2020).
- 610 14 Folegatti, P. M. *et al.* Safety and immunogenicity of the ChAdOx1 nCoV-19 vaccine
611 against SARS-CoV-2: a preliminary report of a phase 1/2, single-blind, randomised
612 controlled trial. *Lancet* **396**, 467-478, doi:10.1016/S0140-6736(20)31604-4 (2020).
- 613 15 Kemp, S. A. *et al.* Recurrent emergence and transmission of a SARS-CoV-2 Spike
614 deletion Δ H69/V70. *bioRxiv*, 2020.2012.2014.422555,
615 doi:10.1101/2020.12.14.422555 (2020).
- 616 16 Tegally, H. *et al.* Emergence and rapid spread of a new severe acute respiratory
617 syndrome-related coronavirus 2 (SARS-CoV-2) lineage with multiple spike mutations
618 in South Africa. *medRxiv*, 2020.2012.2021.20248640,
619 doi:10.1101/2020.12.21.20248640 (2020).

- 620 17 Faria, N. R. *et al.* Genomic characterisation of an emergent SARS-CoV-2 lineage in
621 Manaus: preliminary findings, <[https://virological.org/t/genomic-characterisation-](https://virological.org/t/genomic-characterisation-of-an-emergent-sars-cov-2-lineage-in-manaus-preliminary-findings/586)
622 [of-an-emergent-sars-cov-2-lineage-in-manaus-preliminary-findings/586](https://virological.org/t/genomic-characterisation-of-an-emergent-sars-cov-2-lineage-in-manaus-preliminary-findings/586)> (2021).
- 623 18 Jackson, L. A. *et al.* An mRNA Vaccine against SARS-CoV-2 - Preliminary Report. *N*
624 *Engl J Med* **383**, 1920-1931, doi:10.1056/NEJMoa2022483 (2020).
- 625 19 Walsh, E. E. *et al.* Safety and Immunogenicity of Two RNA-Based Covid-19 Vaccine
626 Candidates. *New England Journal of Medicine* **383**, 2439-2450,
627 doi:10.1056/NEJMoa2027906 (2020).
- 628 20 Schmidt, F. *et al.* Measuring SARS-CoV-2 neutralizing antibody activity using
629 pseudotyped and chimeric viruses. 2020.2006.2008.140871,
630 doi:10.1101/2020.06.08.140871 %J bioRxiv (2020).
- 631 21 Brouwer, P. J. M. *et al.* Potent neutralizing antibodies from COVID-19 patients define
632 multiple targets of vulnerability. *Science* **369**, 643-650, doi:10.1126/science.abc5902
633 (2020).
- 634 22 Wang, P. L., L; Iketani, S, Luo, Y; Guo, Y; Ho, D. Increased Resistance of SARS-CoV-2
635 Variants B.1.351 and B.1.1.7 to Antibody Neutralization. *bioRxiv* (2021).
- 636 23 PHE. *Public Health England statement on Variant of Concern and new Variant Under*
637 *Investigation*, <[https://www.gov.uk/government/news/phe-statement-on-variant-](https://www.gov.uk/government/news/phe-statement-on-variant-of-concern-and-new-variant-under-investigation)
638 [of-concern-and-new-variant-under-investigation](https://www.gov.uk/government/news/phe-statement-on-variant-of-concern-and-new-variant-under-investigation)> (2021).
- 639 24 McCallum, M. *et al.* N-terminal domain antigenic mapping reveals a site of
640 vulnerability for SARS-CoV-2. *bioRxiv*, doi:10.1101/2021.01.14.426475 (2021).
- 641 25 Thomson, E. C. *et al.* Circulating SARS-CoV-2 spike N439K variants maintain fitness
642 while evading antibody-mediated immunity. *Cell*, doi:10.1016/j.cell.2021.01.037
643 (2021).
- 644 26 Greaney, A. J. *et al.* Comprehensive mapping of mutations to the SARS-CoV-2
645 receptor-binding domain that affect recognition by polyclonal human serum
646 antibodies. *Cell host & microbe*, doi:<https://doi.org/10.1016/j.chom.2021.02.003>
647 (2021).
- 648 27 Andreano, E. *et al.* SARS-CoV-2 escape in vitro from a highly neutralizing
649 COVID-19 convalescent plasma. *bioRxiv*, 2020.2012.2028.424451,
650 doi:10.1101/2020.12.28.424451 (2020).
- 651 28 Walls, A. C. *et al.* Structure, Function, and Antigenicity of the SARS- CoV-2 Spike
652 Glycoprotein. *Cell* **181**, 281-292.e286,
653 doi:papers3://publication/doi/10.1016/j.cell.2020.02.058 (2020).
- 654 29 Guan, Y. *et al.* Isolation and characterization of viruses related to the SARS
655 coronavirus from animals in southern China. *Science* **302**, 276-278,
656 doi:10.1126/science.1087139 (2003).
- 657 30 Li, W. *et al.* Efficient replication of severe acute respiratory syndrome coronavirus in
658 mouse cells is limited by murine angiotensin-converting enzyme 2. *J Virol* **78**, 11429-
659 11433, doi:10.1128/JVI.78.20.11429-11433.2004 (2004).
- 660 31 Li, W. *et al.* Receptor and viral determinants of SARS-coronavirus adaptation to
661 human ACE2. *The EMBO journal* **24**, 1634-1643 (2005).
- 662 32 Starr, T. N. *et al.* Deep Mutational Scanning of SARS-CoV-2 Receptor Binding Domain
663 Reveals Constraints on Folding and ACE2 Binding. *Cell* **182**, 1295-1310 e1220,
664 doi:10.1016/j.cell.2020.08.012 (2020).
- 665 33 Wang, Z. *et al.* mRNA vaccine-elicited antibodies to SARS-CoV-2 and circulating
666 variants. *Nature*, doi:10.1038/s41586-021-03324-6 (2021).

667 34 Wibmer, C. K. *et al.* SARS-CoV-2 501Y.V2 escapes neutralization by South African
668 COVID-19 donor plasma. *bioRxiv*, doi:10.1101/2021.01.18.427166 (2021).

669 35 Verschoor, C. P. *et al.* Microneutralization assay titres correlate with protection
670 against seasonal influenza H1N1 and H3N2 in children. *PloS one* **10**, e0131531,
671 doi:10.1371/journal.pone.0131531 (2015).

672 36 Kulkarni, P. S., Hurwitz, J. L., Simoes, E. A. F. & Piedra, P. A. Establishing Correlates of
673 Protection for Vaccine Development: Considerations for the Respiratory Syncytial
674 Virus Vaccine Field. *Viral Immunol* **31**, 195-203, doi:10.1089/vim.2017.0147 (2018).

675 37 Goddard, N. L., Cooke, M. C., Gupta, R. K. & Nguyen-Van-Tam, J. S. Timing of
676 monoclonal antibody for seasonal RSV prophylaxis in the United Kingdom. *Epidemiol
677 Infect* **135**, 159-162, doi:10.1017/S0950268806006601 (2007).

678 38 Mercado, N. B. *et al.* Single-shot Ad26 vaccine protects against SARS-CoV-2 in rhesus
679 macaques. *Nature* **586**, 583-588, doi:10.1038/s41586-020-2607-z (2020).

680 39 McMahan, K. *et al.* Correlates of protection against SARS-CoV-2 in rhesus macaques.
681 *Nature*, doi:10.1038/s41586-020-03041-6 (2020).

682 40 Rathnasinghe, R. *et al.* The N501Y mutation in SARS-CoV-2 spike leads to morbidity
683 in obese and aged mice and is neutralized by convalescent and post-vaccination
684 human sera. *medRxiv*, 2021.2001.2019.21249592,
685 doi:10.1101/2021.01.19.21249592 (2021).

686 41 Wang, Z. *et al.* mRNA vaccine-elicited antibodies to SARS-CoV-2 and circulating
687 variants. *bioRxiv*, doi:10.1101/2021.01.15.426911 (2021).

688 42 Muik, A. *et al.* Neutralization of SARS-CoV-2 lineage B.1.1.7 pseudovirus by
689 BNT162b2 vaccine-elicited human sera. *Science*, doi:10.1126/science.abg6105
690 (2021).

691 43 Wu, K. *et al.* mRNA-1273 vaccine induces neutralizing antibodies against spike
692 mutants from global SARS-CoV-2 variants. *bioRxiv*, doi:10.1101/2021.01.25.427948
693 (2021).

694 44 Xie, X. *et al.* Neutralization of N501Y mutant SARS-CoV-2 by BNT162b2 vaccine-
695 elicited sera. *bioRxiv*, 2021.2001.2007.425740, doi:10.1101/2021.01.07.425740
696 (2021).

697 45 Suryadevara, N. *et al.* Neutralizing and protective human monoclonal antibodies
698 recognizing the N-terminal domain of the SARS-CoV-2 spike protein. *bioRxiv*,
699 2021.2001.2019.427324, doi:10.1101/2021.01.19.427324 (2021).

700 46 Soh, W. T. *et al.* The N-terminal domain of spike glycoprotein mediates SARS-CoV-2
701 infection by associating with L-SIGN and DC-SIGN. *bioRxiv*, 1-30,
702 doi:papers3://publication/doi/10.1101/2020.11.05.369264 (2020).

703 47 Greaney, A. J. *et al.* Comprehensive mapping of mutations to the SARS-CoV-2
704 receptor-binding domain that affect recognition by polyclonal human serum
705 antibodies. *bioRxiv*, 2020.2012.2031.425021, doi:10.1101/2020.12.31.425021
706 (2021).

707 48 Greaney, A. J. *et al.* Complete mapping of mutations to the SARS-CoV-2 spike
708 receptor-binding domain that escape antibody recognition. *Cell Host & Microbe*
709 (2020).

710 49 Weisblum, Y. *et al.* Escape from neutralizing antibodies by SARS-CoV-2 spike protein
711 variants. *Elife* **9**, e61312, doi:10.7554/eLife.61312 (2020).

- 712 50 Corti, D. *et al.* A neutralizing antibody selected from plasma cells that binds to group
713 1 and group 2 influenza A hemagglutinins. *Science* **333**, 850-856,
714 doi:10.1126/science.1205669 (2011).
- 715 51 Pinto, D. *et al.* Cross-neutralization of SARS-CoV-2 by a human monoclonal SARS-CoV
716 antibody. *Nature* **583**, 290-295, doi:10.1038/s41586-020-2349-y (2020).
- 717 52 Tortorici, M. A. *et al.* Ultrapotent human antibodies protect against SARS-CoV-2
718 challenge via multiple mechanisms. *Science*, doi:10.1126/science.abe3354 (2020).
- 719 53 Gregson, J. *et al.* HIV-1 viral load is elevated in individuals with reverse transcriptase
720 mutation M184V/I during virological failure of first line antiretroviral therapy and is
721 associated with compensatory mutation L74I. *Journal of Infectious Diseases* (2019).
- 722 54 Forloni, M., Liu, A. Y. & Wajapeyee, N. Creating Insertions or Deletions Using Overlap
723 Extension Polymerase Chain Reaction (PCR) Mutagenesis. *Cold Spring Harb Protoc*
724 **2018**, doi:10.1101/pdb.prot097758 (2018).
- 725 55 Case, J. B. *et al.* Neutralizing Antibody and Soluble ACE2 Inhibition of a Replication-
726 Competent VSV-SARS-CoV-2 and a Clinical Isolate of SARS-CoV-2. *Cell Host Microbe*
727 **28**, 475-485 e475, doi:10.1016/j.chom.2020.06.021 (2020).
- 728 56 Naldini, L., Blomer, U., Gage, F. H., Trono, D. & Verma, I. M. Efficient transfer,
729 integration, and sustained long-term expression of the transgene in adult rat brains
730 injected with a lentiviral vector. *Proceedings of the National Academy of Sciences of*
731 *the United States of America* **93**, 11382-11388 (1996).
- 732 57 Gupta, R. K. *et al.* Full length HIV-1 gag determines protease inhibitor susceptibility
733 within in vitro assays. *AIDS* **24**, 1651 (2010).
- 734 58 Mlcochova, P. *et al.* Combined point of care nucleic acid and antibody testing for
735 SARS-CoV-2 following emergence of D614G Spike Variant. *Cell Rep Med*, 100099,
736 doi:10.1016/j.xcrm.2020.100099 (2020).
- 737 59 Walls, A. C. *et al.* Elicitation of Potent Neutralizing Antibody Responses by Designed
738 Protein Nanoparticle Vaccines for SARS-CoV-2. *Cell* **183**, 1367-1382 e1317,
739 doi:10.1016/j.cell.2020.10.043 (2020).
- 740 60 Chi, X. *et al.* A neutralizing human antibody binds to the N-terminal domain of the
741 Spike protein of SARS-CoV-2. *Science*, eabc6952-6913,
742 doi:papers3://publication/doi/10.1126/science.abc6952 (2020).
- 743 61 Tortorici, M. A. *et al.* Ultrapotent human antibodies protect against SARS-CoV-2
744 challenge via multiple mechanisms. *Science* **4**, eabe3354-3316,
745 doi:papers3://publication/doi/10.1126/science.abe3354 (2020).
- 746 62 Piccoli, L. *et al.* Mapping neutralizing and immunodominant sites on the SARS-CoV-2
747 spike receptor-binding domain by structure-guided high-resolution serology. *Cell*, 1-
748 55, doi:papers3://publication/doi/10.1016/j.cell.2020.09.037 (2020).

749

750

751

752 **The COVID-19 Genomics UK (COG-UK) Consortium**

753 **Funding acquisition, Leadership and supervision, Metadata curation, Project**
754 **administration, Samples and logistics, Sequencing and analysis, Software and analysis**
755 **tools, and Visualisation:**

756 Samuel C Robson ¹³.

757
758 **Funding acquisition, Leadership and supervision, Metadata curation, Project**
759 **administration, Samples and logistics, Sequencing and analysis, and Software and analysis**
760 **tools:**
761 Nicholas J Loman ⁴¹ and Thomas R Connor ^{10, 69}.
762
763 **Leadership and supervision, Metadata curation, Project administration, Samples and**
764 **logistics, Sequencing and analysis, Software and analysis tools, and Visualisation:**
765 Tanya Golubchik ⁵.
766
767 **Funding acquisition, Metadata curation, Samples and logistics, Sequencing and analysis,**
768 **Software and analysis tools, and Visualisation:**
769 Rocio T Martinez Nunez ⁴².
770
771 **Funding acquisition, Leadership and supervision, Metadata curation, Project**
772 **administration, and Samples and logistics:**
773 Catherine Ludden ⁸⁸.
774
775 **Funding acquisition, Leadership and supervision, Metadata curation, Samples and**
776 **logistics, and Sequencing and analysis:**
777 Sally Corden ⁶⁹.
778
779 **Funding acquisition, Leadership and supervision, Project administration, Samples and**
780 **logistics, and Sequencing and analysis:**
781 Ian Johnston ⁹⁹ and David Bonsall ⁵.
782
783 **Funding acquisition, Leadership and supervision, Sequencing and analysis, Software and**
784 **analysis tools, and Visualisation:**
785 Colin P Smith ⁸⁷ and Ali R Awan ²⁸.
786
787 **Funding acquisition, Samples and logistics, Sequencing and analysis, Software and analysis**
788 **tools, and Visualisation:**
789 Giselda Bucca ⁸⁷.
790
791 **Leadership and supervision, Metadata curation, Project administration, Samples and**
792 **logistics, and Sequencing and analysis:**
793 M. Estee Torok ^{22, 101}.
794
795 **Leadership and supervision, Metadata curation, Project administration, Samples and**
796 **logistics, and Visualisation:**
797 Kordo Saeed ^{81, 110} and Jacqui A Prieto ^{83, 109}.
798
799 **Leadership and supervision, Metadata curation, Project administration, Sequencing and**
800 **analysis, and Software and analysis tools:**
801 David K Jackson ⁹⁹.
802

803 **Metadata curation, Project administration, Samples and logistics, Sequencing and**
804 **analysis, and Software and analysis tools:**
805 William L Hamilton ²².
806 **Metadata curation, Project administration, Samples and logistics, Sequencing and**
807 **analysis, and Visualisation:**
808 Luke B Snell ¹¹.
809
810 **Funding acquisition, Leadership and supervision, Metadata curation, and Samples and**
811 **logistics:**
812 Catherine Moore ⁶⁹.
813
814 **Funding acquisition, Leadership and supervision, Project administration, and Samples and**
815 **logistics:**
816 Ewan M Harrison ^{99, 88}.
817
818 **Leadership and supervision, Metadata curation, Project administration, and Samples and**
819 **logistics:**
820 Sonia Goncalves ⁹⁹.
821
822 **Leadership and supervision, Metadata curation, Samples and logistics, and Sequencing**
823 **and analysis:**
824 Ian G Goodfellow ²⁴, Derek J Fairley ^{3, 72}, Matthew W Loose ¹⁸ and Joanne Watkins ⁶⁹.
825
826 **Leadership and supervision, Metadata curation, Samples and logistics, and Software and**
827 **analysis tools:**
828 Rich Livett ⁹⁹.
829
830 **Leadership and supervision, Metadata curation, Samples and logistics, and Visualisation:**
831 Samuel Moses ^{25, 106}.
832
833 **Leadership and supervision, Metadata curation, Sequencing and analysis, and Software**
834 **and analysis tools:**
835 Roberto Amato ⁹⁹, Sam Nicholls ⁴¹ and Matthew Bull ⁶⁹.
836
837 **Leadership and supervision, Project administration, Samples and logistics, and Sequencing**
838 **and analysis:**
839 Darren L Smith ^{37, 58, 105}.
840
841 **Leadership and supervision, Sequencing and analysis, Software and analysis tools, and**
842 **Visualisation:**
843 Jeff Barrett ⁹⁹, David M Aanensen ^{14, 114}.
844
845 **Metadata curation, Project administration, Samples and logistics, and Sequencing and**
846 **analysis:**
847 Martin D Curran ⁶⁵, Surendra Parmar ⁶⁵, Dinesh Aggarwal ^{95, 99, 64} and James G Shepherd ⁴⁸.
848

849 **Metadata curation, Project administration, Sequencing and analysis, and Software and**
850 **analysis tools:**
851 Matthew D Parker ⁹³.
852

853 **Metadata curation, Samples and logistics, Sequencing and analysis, and Visualisation:**
854 Sharon Glaysher ⁶¹.
855

856 **Metadata curation, Sequencing and analysis, Software and analysis tools, and**
857 **Visualisation:**
858 Matthew Bashton ^{37, 58}, Anthony P Underwood ^{14, 114}, Nicole Pacchiarini ⁶⁹ and Katie F
859 Loveson ⁷⁷.
860

861

862 **Project administration, Sequencing and analysis, Software and analysis tools, and**
863 **Visualisation:**
864 Alessandro M Carabelli ⁸⁸.
865

866 **Funding acquisition, Leadership and supervision, and Metadata curation:**
867 Kate E Templeton ^{53, 90}.
868

869 **Funding acquisition, Leadership and supervision, and Project administration:**
870 Cordelia F Langford ⁹⁹, John Sillitoe ⁹⁹, Thushan I de Silva ⁹³ and Dennis Wang ⁹³.
871

872 **Funding acquisition, Leadership and supervision, and Sequencing and analysis:**
873 Dominic Kwiatkowski ^{99, 107}, Andrew Rambaut ⁹⁰, Justin O'Grady ^{70, 89} and Simon Cottrell ⁶⁹.
874

875 **Leadership and supervision, Metadata curation, and Sequencing and analysis:**
876 Matthew T.G. Holden ⁶⁸ and Emma C Thomson ⁴⁸.
877

878 **Leadership and supervision, Project administration, and Samples and logistics:**
879 Husam Osman ^{64, 36}, Monique Andersson ⁵⁹, Anoop J Chauhan ⁶¹ and Mohammed O Hassan-
880 Ibrahim ⁶.
881

882 **Leadership and supervision, Project administration, and Sequencing and analysis:**
883 Mara Lawniczak ⁹⁹.
884

885 **Leadership and supervision, Samples and logistics, and Sequencing and analysis:**
886 Ravi Kumar Gupta ^{88, 113}, Alex Alderton ⁹⁹, Meera Chand ⁶⁶, Chrystala Constantinidou ⁹⁴,
887 Meera Unnikrishnan ⁹⁴, Alistair C Darby ⁹², Julian A Hiscox ⁹² and Steve Paterson ⁹².
888

889 **Leadership and supervision, Sequencing and analysis, and Software and analysis tools:**
890 Inigo Martincorena ⁹⁹, David L Robertson ⁴⁸, Erik M Volz ³⁹, Andrew J Page ⁷⁰ and Oliver G
891 Pybus ²³.
892

893 **Leadership and supervision, Sequencing and analysis, and Visualisation:**
894 Andrew R Bassett ⁹⁹.
895

896 **Metadata curation, Project administration, and Samples and logistics:**
897 Cristina V Ariani ⁹⁹, Michael H Spencer Chapman ^{99, 88}, Kathy K Li ⁴⁸, Rajiv N Shah ⁴⁸, Natasha
898 G Jesudason ⁴⁸ and Yusri Taha ⁵⁰.
899

900 **Metadata curation, Project administration, and Sequencing and analysis:**
901 Martin P McHugh ⁵³ and Rebecca Dewar ⁵³.
902

903 **Metadata curation, Samples and logistics, and Sequencing and analysis:**
904 Aminu S Jahun ²⁴, Claire McMurray ⁴¹, Sarojini Pandey ⁸⁴, James P McKenna ³, Andrew
905 Nelson ^{58, 105}, Gregory R Young ^{37, 58}, Clare M McCann ^{58, 105} and Scott Elliott ⁶¹.
906

907 **Metadata curation, Samples and logistics, and Visualisation:**
908 Hannah Lowe ²⁵.
909

910 **Metadata curation, Sequencing and analysis, and Software and analysis tools:**
911 Ben Temperton ⁹¹, Sunando Roy ⁸², Anna Price ¹⁰, Sara Rey ⁶⁹ and Matthew Wyles ⁹³.
912

913 **Metadata curation, Sequencing and analysis, and Visualisation:**
914 Stefan Rooke ⁹⁰ and Sharif Shaaban ⁶⁸.
915
916

917 **Project administration, Samples and logistics, Sequencing and analysis:**
918 Mariateresa de Cesare ⁹⁸.
919

920 **Project administration, Samples and logistics, and Software and analysis tools:**
921 Laura Letchford ⁹⁹.
922

923 **Project administration, Samples and logistics, and Visualisation:**
924 Siona Silveira ⁸¹, Emanuela Pelosi ⁸¹ and Eleri Wilson-Davies ⁸¹.
925

926 **Samples and logistics, Sequencing and analysis, and Software and analysis tools:**
927 Myra Hosmillo ²⁴.
928

929 **Sequencing and analysis, Software and analysis tools, and Visualisation:**
930 Áine O'Toole ⁹⁰, Andrew R Hesketh ⁸⁷, Richard Stark ⁹⁴, Louis du Plessis ²³, Chris Ruis ⁸⁸, Helen
931 Adams ⁴ and Yann Bourgeois ⁷⁶.
932

933 **Funding acquisition, and Leadership and supervision:**
934 Stephen L Michell ⁹¹, Dimitris Gramatopoulos ^{84, 112}, Jonathan Edgeworth ¹², Judith Breuer ^{30,}
935 ⁸², John A Todd ⁹⁸ and Christophe Fraser ⁵.
936

937 **Funding acquisition, and Project administration:**
938 David Buck ⁹⁸ and Michaela John ⁹.
939

940 **Leadership and supervision, and Metadata curation:**
941 Gemma L Kay ⁷⁰.
942

943 **Leadership and supervision, and Project administration:**
944 Steve Palmer⁹⁹, Sharon J Peacock^{88, 64} and David Heyburn⁶⁹.
945

946 **Leadership and supervision, and Samples and logistics:**
947 Danni Weldon⁹⁹, Esther Robinson^{64, 36}, Alan McNally^{41, 86}, Peter Muir⁶⁴, Ian B Vipond⁶⁴,
948 John BoYes²⁹, Venkat Sivaprakasam⁴⁶, Tranpriet Salluja⁷⁵, Samir Dervisevic⁵⁴ and Emma J
949 Meader⁵⁴.
950

951 **Leadership and supervision, and Sequencing and analysis:**
952 Naomi R Park⁹⁹, Karen Oliver⁹⁹, Aaron R Jeffries⁹¹, Sascha Ott⁹⁴, Ana da Silva Filipe⁴⁸,
953 David A Simpson⁷² and Chris Williams⁶⁹.
954

955 **Leadership and supervision, and Visualisation:**
956 Jane AH Masoli^{73, 91}.
957

958 **Metadata curation, and Samples and logistics:**
959 Bridget A Knight^{73, 91}, Christopher R Jones^{73, 91}, Cherian Koshy¹, Amy Ash¹, Anna Casey⁷¹,
960 Andrew Bosworth^{64, 36}, Liz Ratcliffe⁷¹, Li Xu-McCrae³⁶, Hannah M Pymont⁶⁴, Stephanie
961 Hutchings⁶⁴, Lisa Berry⁸⁴, Katie Jones⁸⁴, Fenella Halstead⁴⁶, Thomas Davis²¹, Christopher
962 Holmes¹⁶, Miren Iturriza-Gomara⁹², Anita O Lucaci⁹², Paul Anthony Randell^{38, 104}, Alison
963 Cox^{38, 104}, Pinglawathee Madona^{38, 104}, Kathryn Ann Harris³⁰, Julianne Rose Brown³⁰,
964 Tabitha W Mahungu⁷⁴, Dianne Irish-Tavares⁷⁴, Tanzina Haque⁷⁴, Jennifer Hart⁷⁴, Eric
965 Witele⁷⁴, Melisa Louise Fenton⁷⁵, Steven Liggett⁷⁹, Clive Graham⁵⁶, Emma Swindells⁵⁷,
966 Jennifer Collins⁵⁰, Gary Eltringham⁵⁰, Sharon Campbell¹⁷, Patrick C McClure⁹⁷, Gemma
967 Clark¹⁵, Tim J Sloan⁶⁰, Carl Jones¹⁵ and Jessica Lynch^{2, 111}.
968
969
970

971 **Metadata curation, and Sequencing and analysis:**
972 Ben Warne⁸, Steven Leonard⁹⁹, Jillian Durham⁹⁹, Thomas Williams⁹⁰, Sam T Haldenby⁹²,
973 Nathaniel Storey³⁰, Nabil-Fareed Alikhan⁷⁰, Nadine Holmes¹⁸, Christopher Moore¹⁸,
974 Matthew Carlile¹⁸, Malorie Perry⁶⁹, Noel Craine⁶⁹, Ronan A Lyons⁸⁰, Angela H Beckett¹³,
975 Salman Goudarzi⁷⁷, Christopher Fearn⁷⁷, Kate Cook⁷⁷, Hannah Dent⁷⁷ and Hannah Paul⁷⁷.
976

977 **Metadata curation, and Software and analysis tools:**
978 Robert Davies⁹⁹.
979

980 **Project administration, and Samples and logistics:**
981 Beth Blane⁸⁸, Sophia T Girgis⁸⁸, Mathew A Beale⁹⁹, Katherine L Bellis^{99, 88}, Matthew J
982 Dorman⁹⁹, Eleanor Drury⁹⁹, Leanne Kane⁹⁹, Sally Kay⁹⁹, Samantha McGuigan⁹⁹, Rachel
983 Nelson⁹⁹, Liam Prestwood⁹⁹, Shavanthi Rajatileka⁹⁹, Rahul Batra¹², Rachel J Williams⁸²,
984 Mark Kristiansen⁸², Angie Green⁹⁸, Anita Justice⁵⁹, Adhyana I.K Mahanama^{81, 102} and
985 Buddhini Samaraweera^{81, 102}.
986

987 **Project administration, and Sequencing and analysis:**
988 Nazreen F Hadjirin⁸⁸ and Joshua Quick⁴¹.
989

990 **Project administration, and Software and analysis tools:**
991 Radoslaw Poplawski ⁴¹.
992
993 **Samples and logistics, and Sequencing and analysis:**
994 Leanne M Kermack ⁸⁸, Nicola Reynolds ⁷, Grant Hall ²⁴, Yasmin Chaudhry ²⁴, Malte L Pinckert
995 ²⁴, Iliana Georgana ²⁴, Robin J Moll ⁹⁹, Alicia Thornton ⁶⁶, Richard Myers ⁶⁶, Joanne Stockton
996 ⁴¹, Charlotte A Williams ⁸², Wen C Yew ⁵⁸, Alexander J Trotter ⁷⁰, Amy Trebes ⁹⁸, George
997 MacIntyre-Cockett ⁹⁸, Alec Birchley ⁶⁹, Alexander Adams ⁶⁹, Amy Plimmer ⁶⁹, Bree Gatica-
998 Wilcox ⁶⁹, Caoimhe McKerr ⁶⁹, Ember Hilvers ⁶⁹, Hannah Jones ⁶⁹, Hibo Asad ⁶⁹, Jason
999 Coombes ⁶⁹, Johnathan M Evans ⁶⁹, Laia Fina ⁶⁹, Lauren Gilbert ⁶⁹, Lee Graham ⁶⁹, Michelle
1000 Cronin ⁶⁹, Sara Kumziene-SummerhaYes ⁶⁹, Sarah Taylor ⁶⁹, Sophie Jones ⁶⁹, Danielle C
1001 Groves ⁹³, Peijun Zhang ⁹³, Marta Gallis ⁹³ and Stavroula F Louka ⁹³.
1002
1003 **Samples and logistics, and Software and analysis tools:**
1004 Igor Starinskij ⁴⁸.
1005
1006 **Sequencing and analysis, and Software and analysis tools:**
1007 Chris J Illingworth ⁴⁷, Chris Jackson ⁴⁷, Marina Gourtovaia ⁹⁹, Gerry Tonkin-Hill ⁹⁹, Kevin Lewis
1008 ⁹⁹, Jaime M Tovar-Corona ⁹⁹, Keith James ⁹⁹, Laura Baxter ⁹⁴, Mohammad T. Alam ⁹⁴, Richard
1009 J Orton ⁴⁸, Joseph Hughes ⁴⁸, Sreenu Vattipally ⁴⁸, Manon Ragonnet-Cronin ³⁹, Fabricia F.
1010 Nascimento ³⁹, David Jorgensen ³⁹, Olivia Boyd ³⁹, Lily Geidelberg ³⁹, Alex E Zarebski ²³, Jayna
1011 Raghwani ²³, Moritz UG Kraemer ²³, Joel Southgate ^{10, 69}, Benjamin B Lindsey ⁹³ and Timothy
1012 M Freeman ⁹³.
1013
1014 **Software and analysis tools, and Visualisation:**
1015 Jon-Paul Keatley ⁹⁹, Joshua B Singer ⁴⁸, Leonardo de Oliveira Martins ⁷⁰, Corin A Yeats ¹⁴,
1016 Khalil Abudahab ^{14, 114}, Ben EW Taylor ^{14, 114} and Mirko Menegazzo ¹⁴.
1017
1018 **Leadership and supervision:**
1019 John Danesh ⁹⁹, Wendy Hogsden ⁴⁶, Sahar Eldirdiri ²¹, Anita Kenyon ²¹, Jenifer Mason ⁴³,
1020 Trevor I Robinson ⁴³, Alison Holmes ^{38, 103}, James Price ^{38, 103}, John A Hartley ⁸², Tanya Curran
1021 ³, Alison E Mather ⁷⁰, Giri Shankar ⁶⁹, Rachel Jones ⁶⁹, Robin Howe ⁶⁹ and Sian Morgan ⁹.
1022
1023
1024
1025 **Metadata curation:**
1026 Elizabeth Wastenge ⁵³, Michael R Chapman ^{34, 88, 99}, Siddharth Mookerjee ^{38, 103}, Rachael
1027 Stanley ⁵⁴, Wendy Smith ¹⁵, Timothy Peto ⁵⁹, David Eyre ⁵⁹, Derrick Crook ⁵⁹, Gabrielle Vernet
1028 ³³, Christine Kitchen ¹⁰, Huw Gulliver ¹⁰, Ian Merrick ¹⁰, Martyn Guest ¹⁰, Robert Munn ¹⁰,
1029 Declan T Bradley ^{63, 72} and Tim Wyatt ⁶³.
1030
1031 **Project administration:**
1032 Charlotte Beaver ⁹⁹, Luke Foulser ⁹⁹, Sophie Palmer ⁸⁸, Carol M Churcher ⁸⁸, Ellena Brooks ⁸⁸,
1033 Kim S Smith ⁸⁸, Katerina Galai ⁸⁸, Georgina M McManus ⁸⁸, Frances Bolt ^{38, 103}, Francesc Coll
1034 ¹⁹, Lizzie Meadows ⁷⁰, Stephen W Attwood ²³, Alisha Davies ⁶⁹, Elen De Lacy ⁶⁹, Fatima
1035 Downing ⁶⁹, Sue Edwards ⁶⁹, Garry P Scarlett ⁷⁶, Sarah Jeremiah ⁸³ and Nikki Smith ⁹³.
1036

1037 **Samples and logistics:**
1038 Danielle Leek⁸⁸, Sushmita Sridhar^{88, 99}, Sally Forrest⁸⁸, Claire Cormie⁸⁸, Harmeet K Gill⁸⁸,
1039 Joana Dias⁸⁸, Ellen E Higginson⁸⁸, Mailis Maes⁸⁸, Jamie Young⁸⁸, Michelle Wantoch⁷,
1040 Sanger Covid Team (www.sanger.ac.uk/covid-team)⁹⁹, Dorota Jamroz⁹⁹, Stephanie Lo⁹⁹,
1041 Minal Patel⁹⁹, Verity Hill⁹⁰, Claire M Bewshea⁹¹, Sian Ellard^{73, 91}, Cressida Auckland⁷³, Ian
1042 Harrison⁶⁶, Chloe Bishop⁶⁶, Vicki Chalker⁶⁶, Alex Richter⁸⁵, Andrew Beggs⁸⁵, Angus Best⁸⁶,
1043 Benita Percival⁸⁶, Jeremy Mirza⁸⁶, Oliver Megram⁸⁶, Megan Mayhew⁸⁶, Liam Crawford⁸⁶,
1044 Fiona Ashcroft⁸⁶, Emma Moles-Garcia⁸⁶, Nicola Cumley⁸⁶, Richard Hopes⁶⁴, Patawee
1045 Asamaphan⁴⁸, Marc O Niebel⁴⁸, Rory N Gunson¹⁰⁰, Amanda Bradley⁵², Alasdair Maclean⁵²,
1046 Guy Mollett⁵², Rachel Blacow⁵², Paul Bird¹⁶, Thomas Helmer¹⁶, Karlie Fallon¹⁶, Julian Tang
1047¹⁶, Antony D Hale⁴⁹, Louissa R Macfarlane-Smith⁴⁹, Katherine L Harper⁴⁹, Holli Carden⁴⁹,
1048 Nicholas W Machin^{45, 64}, Kathryn A Jackson⁹², Shazaad S Y Ahmad^{45, 64}, Ryan P George⁴⁵,
1049 Lance Turtle⁹², Elaine O'Toole⁴³, Joanne Watts⁴³, Cassie Breen⁴³, Angela Cowell⁴³, Adela
1050 Alcolea-Medina^{32, 96}, Themoula Charalampous^{12, 42}, Amita Patel¹¹, Lisa J Levett³⁵, Judith
1051 Heaney³⁵, Aileen Rowan³⁹, Graham P Taylor³⁹, Divya Shah³⁰, Laura Atkinson³⁰, Jack CD Lee
1052³⁰, Adam P Westhorpe⁸², Riaz Jannoo⁸², Helen L Lowe⁸², Angeliki Karamani⁸², Leah Ensell
1053⁸², Wendy Chatterton³⁵, Monika Pusok³⁵, Ashok Dadrah⁷⁵, Amanda Symmonds⁷⁵, Graciela
1054 Sluga⁴⁴, Zoltan Molnar⁷², Paul Baker⁷⁹, Stephen Bonner⁷⁹, Sarah Essex⁷⁹, Edward Barton
1055⁵⁶, Debra Padgett⁵⁶, Garren Scott⁵⁶, Jane Greenaway⁵⁷, Brendan Al Payne⁵⁰, Shirelle
1056 Burton-Fanning⁵⁰, Sheila Waugh⁵⁰, Veena Raviprakash¹⁷, Nicola Sheriff¹⁷, Victoria Blakey
1057¹⁷, Lesley-Anne Williams¹⁷, Jonathan Moore²⁷, Susanne Stonehouse²⁷, Louise Smith⁵⁵, Rose
1058 K Davidson⁸⁹, Luke Bedford²⁶, Lindsay Coupland⁵⁴, Victoria Wright¹⁸, Joseph G Chappell⁹⁷,
1059 Theocharis Tsoleridis⁹⁷, Jonathan Ball⁹⁷, Manjinder Khakh¹⁵, Vicki M Fleming¹⁵, Michelle M
1060 Lister¹⁵, Hannah C Howson-Wells¹⁵, Louise Berry¹⁵, Tim Boswell¹⁵, Amelia Joseph¹⁵, Iona
1061 Willingham¹⁵, Nichola Duckworth⁶⁰, Sarah Walsh⁶⁰, Emma Wise^{2, 111}, Nathan Moore^{2, 111},
1062 Matilde Mori^{2, 108, 111}, Nick Cortes^{2, 111}, Stephen Kidd^{2, 111}, Rebecca Williams³³, Laura
1063 Gifford⁶⁹, Kelly Bicknell⁶¹, Sarah Wyllie⁶¹, Allyson Lloyd⁶¹, Robert Impey⁶¹, Cassandra S
1064 Malone⁶, Benjamin J Cogger⁶, Nick Levene⁶², Lynn Monaghan⁶², Alexander J Keeley⁹³,
1065 David G Partridge^{78, 93}, Mohammad Raza^{78, 93}, Cariad Evans^{78, 93} and Kate Johnson^{78, 93}.

1066
1067 **Sequencing and analysis:**
1068 Emma Betteridge⁹⁹, Ben W Farr⁹⁹, Scott Goodwin⁹⁹, Michael A Quail⁹⁹, Carol Scott⁹⁹,
1069 Lesley Shirley⁹⁹, Scott AJ Thurston⁹⁹, Diana Rajan⁹⁹, Iraad F Bronner⁹⁹, Louise Aigrain⁹⁹,
1070 Nicholas M Redshaw⁹⁹, Stefanie V Lensing⁹⁹, Shane McCarthy⁹⁹, Alex Makunin⁹⁹, Carlos E
1071 Balcazar⁹⁰, Michael D Gallagher⁹⁰, Kathleen A Williamson⁹⁰, Thomas D Stanton⁹⁰, Michelle
1072 L Michelsen⁹¹, Joanna Warwick-Dugdale⁹¹, Robin Manley⁹¹, Audrey Farbos⁹¹, James W
1073 Harrison⁹¹, Christine M Sambles⁹¹, David J Studholme⁹¹, Angie Lackenby⁶⁶, Tamyo Mbisa
1074⁶⁶, Steven Platt⁶⁶, Shahjahan Miah⁶⁶, David Bibby⁶⁶, Carmen Manso⁶⁶, Jonathan Hubb⁶⁶,
1075 Gavin Dabrera⁶⁶, Mary Ramsay⁶⁶, Daniel Bradshaw⁶⁶, Ulf Schaefer⁶⁶, Natalie Groves⁶⁶,
1076 Eileen Gallagher⁶⁶, David Lee⁶⁶, David Williams⁶⁶, Nicholas Ellaby⁶⁶, Hassan Hartman⁶⁶,
1077 Nikos Manesis⁶⁶, Vineet Patel⁶⁶, Juan Ledesma⁶⁷, Katherine A Twohig⁶⁷, Elias Allara^{64, 88},
1078 Clare Pearson^{64, 88}, Jeffrey K. J. Cheng⁹⁴, Hannah E. Bridgewater⁹⁴, Lucy R. Frost⁹⁴, Grace
1079 Taylor-Joyce⁹⁴, Paul E Brown⁹⁴, Lily Tong⁴⁸, Alice Broos⁴⁸, Daniel Mair⁴⁸, Jenna Nichols⁴⁸,
1080 Stephen N Carmichael⁴⁸, Katherine L Smollett⁴⁰, Kyriaki Nomikou⁴⁸, Elihu Aranday-Cortes
1081⁴⁸, Natasha Johnson⁴⁸, Seema Nickbakhsh^{48, 68}, Edith E Vamos⁹², Margaret Hughes⁹²,
1082 Lucille Rainbow⁹², Richard Eccles⁹², Charlotte Nelson⁹², Mark Whitehead⁹², Richard
1083 Gregory⁹², Matthew Gemmell⁹², Claudia Wierzbicki⁹², Hermione J Webster⁹², Chloe L

1084 Fisher ²⁸, Adrian W Signell ²⁰, Gilberto Betancor ²⁰, Harry D Wilson ²⁰, Gaia Nebbia ¹², Flavia
1085 Flaviani ³¹, Alberto C Cerda ⁹⁶, Tammy V Merrill ⁹⁶, Rebekah E Wilson ⁹⁶, Marius Cotic ⁸²,
1086 Nadua Bayzid ⁸², Thomas Thompson ⁷², Erwan Acheson ⁷², Steven Rushton ⁵¹, Sarah O'Brien
1087 ⁵¹, David J Baker ⁷⁰, Steven Rudder ⁷⁰, Alp Aydin ⁷⁰, Fei Sang ¹⁸, Johnny Debebe ¹⁸, Sarah
1088 Francois ²³, Tetyana I Vasylyeva ²³, Marina Escalera Zamudio ²³, Bernardo Gutierrez ²³,
1089 Angela Marchbank ¹⁰, Joshua Maksimovic ⁹, Karla Spellman ⁹, Kathryn McCluggage ⁹, Mari
1090 Morgan ⁶⁹, Robert Beer ⁹, Safiah Afifi ⁹, Trudy Workman ¹⁰, William Fuller ¹⁰, Catherine
1091 Bresner ¹⁰, Adrienn Angyal ⁹³, Luke R Green ⁹³, Paul J Parsons ⁹³, Rachel M Tucker ⁹³, Rebecca
1092 Brown ⁹³ and Max Whiteley ⁹³.

1093

1094 **Software and analysis tools:**

1095 James Bonfield ⁹⁹, Christoph Puethe ⁹⁹, Andrew Whitwham ⁹⁹, Jennifer Liddle ⁹⁹, Will Rowe
1096 ⁴¹, Igor Siveroni ³⁹, Thanh Le-Viet ⁷⁰ and Amy Gaskin ⁶⁹.

1097

1098 **Visualisation:**

1099 Rob Johnson ³⁹.

1100

1101

1102 **1** Barking, Havering and Redbridge University Hospitals NHS Trust, **2** Basingstoke Hospital, **3** Belfast Health &
1103 Social Care Trust, **4** Betsi Cadwaladr University Health Board, **5** Big Data Institute, Nuffield Department of
1104 Medicine, University of Oxford, **6** Brighton and Sussex University Hospitals NHS Trust, **7** Cambridge Stem Cell
1105 Institute, University of Cambridge, **8** Cambridge University Hospitals NHS Foundation Trust, **9** Cardiff and Vale
1106 University Health Board, **10** Cardiff University, **11** Centre for Clinical Infection & Diagnostics Research, St.
1107 Thomas' Hospital and Kings College London, **12** Centre for Clinical Infection and Diagnostics Research,
1108 Department of Infectious Diseases, Guy's and St Thomas' NHS Foundation Trust, **13** Centre for Enzyme
1109 Innovation, University of Portsmouth (PORT), **14** Centre for Genomic Pathogen Surveillance, University of
1110 Oxford, **15** Clinical Microbiology Department, Queens Medical Centre, **16** Clinical Microbiology, University
1111 Hospitals of Leicester NHS Trust, **17** County Durham and Darlington NHS Foundation Trust, **18** Deep Seq, School
1112 of Life Sciences, Queens Medical Centre, University of Nottingham, **19** Department of Infection Biology, Faculty
1113 of Infectious & Tropical Diseases, London School of Hygiene & Tropical Medicine, **20** Department of Infectious
1114 Diseases, King's College London, **21** Department of Microbiology, Kettering General Hospital, **22** Departments
1115 of Infectious Diseases and Microbiology, Cambridge University Hospitals NHS Foundation Trust; Cambridge, UK,
1116 **23** Department of Zoology, University of Oxford, **24** Division of Virology, Department of Pathology, University of
1117 Cambridge, **25** East Kent Hospitals University NHS Foundation Trust, **26** East Suffolk and North Essex NHS
1118 Foundation Trust, **27** Gateshead Health NHS Foundation Trust, **28** Genomics Innovation Unit, Guy's and St.
1119 Thomas' NHS Foundation Trust, **29** Gloucestershire Hospitals NHS Foundation Trust, **30** Great Ormond Street
1120 Hospital for Children NHS Foundation Trust, **31** Guy's and St. Thomas' BRC, **32** Guy's and St. Thomas' Hospitals,
1121 **33** Hampshire Hospitals NHS Foundation Trust, **34** Health Data Research UK Cambridge, **35** Health Services
1122 Laboratories, **36** Heartlands Hospital, Birmingham, **37** Hub for Biotechnology in the Built Environment,
1123 Northumbria University, **38** Imperial College Hospitals NHS Trust, **39** Imperial College London, **40** Institute of
1124 Biodiversity, Animal Health & Comparative Medicine, **41** Institute of Microbiology and Infection, University of
1125 Birmingham, **42** King's College London, **43** Liverpool Clinical Laboratories, **44** Maidstone and Tunbridge Wells

1126 NHS Trust, **45** Manchester University NHS Foundation Trust, **46** Microbiology Department, Wye Valley NHS Trust,
1127 Hereford, **47** MRC Biostatistics Unit, University of Cambridge, **48** MRC-University of Glasgow Centre for Virus
1128 Research, **49** National Infection Service, PHE and Leeds Teaching Hospitals Trust, **50** Newcastle Hospitals NHS
1129 Foundation Trust, **51** Newcastle University, **52** NHS Greater Glasgow and Clyde, **53** NHS Lothian, **54** Norfolk and
1130 Norwich University Hospital, **55** Norfolk County Council, **56** North Cumbria Integrated Care NHS Foundation
1131 Trust, **57** North Tees and Hartlepool NHS Foundation Trust, **58** Northumbria University, **59** Oxford University
1132 Hospitals NHS Foundation Trust, **60** PathLinks, Northern Lincolnshire & Goole NHS Foundation Trust, **61**
1133 Portsmouth Hospitals University NHS Trust, **62** Princess Alexandra Hospital Microbiology Dept., **63** Public Health
1134 Agency, **64** Public Health England, **65** Public Health England, Clinical Microbiology and Public Health Laboratory,
1135 Cambridge, UK, **66** Public Health England, Colindale, **67** Public Health England, Colindale, **68** Public Health
1136 Scotland, **69** Public Health Wales NHS Trust, **70** Quadram Institute Bioscience, **71** Queen Elizabeth Hospital, **72**
1137 Queen's University Belfast, **73** Royal Devon and Exeter NHS Foundation Trust, **74** Royal Free NHS Trust, **75**
1138 Sandwell and West Birmingham NHS Trust, **76** School of Biological Sciences, University of Portsmouth (PORT),
1139 **77** School of Pharmacy and Biomedical Sciences, University of Portsmouth (PORT), **78** Sheffield Teaching
1140 Hospitals, **79** South Tees Hospitals NHS Foundation Trust, **80** Swansea University, **81** University Hospitals
1141 Southampton NHS Foundation Trust, **82** University College London, **83** University Hospital Southampton NHS
1142 Foundation Trust, **84** University Hospitals Coventry and Warwickshire, **85** University of Birmingham, **86**
1143 University of Birmingham Turnkey Laboratory, **87** University of Brighton, **88** University of Cambridge, **89**
1144 University of East Anglia, **90** University of Edinburgh, **91** University of Exeter, **92** University of Liverpool, **93**
1145 University of Sheffield, **94** University of Warwick, **95** University of Cambridge, **96** Viapath, Guy's and St Thomas'
1146 NHS Foundation Trust, and King's College Hospital NHS Foundation Trust, **97** Virology, School of Life Sciences,
1147 Queens Medical Centre, University of Nottingham, **98** Wellcome Centre for Human Genetics, Nuffield
1148 Department of Medicine, University of Oxford, **99** Wellcome Sanger Institute, **100** West of Scotland Specialist
1149 Virology Centre, NHS Greater Glasgow and Clyde, **101** Department of Medicine, University of Cambridge, **102**
1150 Ministry of Health, Sri Lanka, **103** NIHR Health Protection Research Unit in HCAI and AMR, Imperial College
1151 London, **104** North West London Pathology, **105** NU-OMICS, Northumbria University, **106** University of Kent,
1152 **107** University of Oxford, **108** University of Southampton, **109** University of Southampton School of Health
1153 Sciences, **110** University of Southampton School of Medicine, **111** University of Surrey, **112** Warwick Medical
1154 School and Institute of Precision Diagnostics, Pathology, UHCW NHS Trust, **113** Wellcome Africa Health Research
1155 Institute Durban
1156

Figure 1

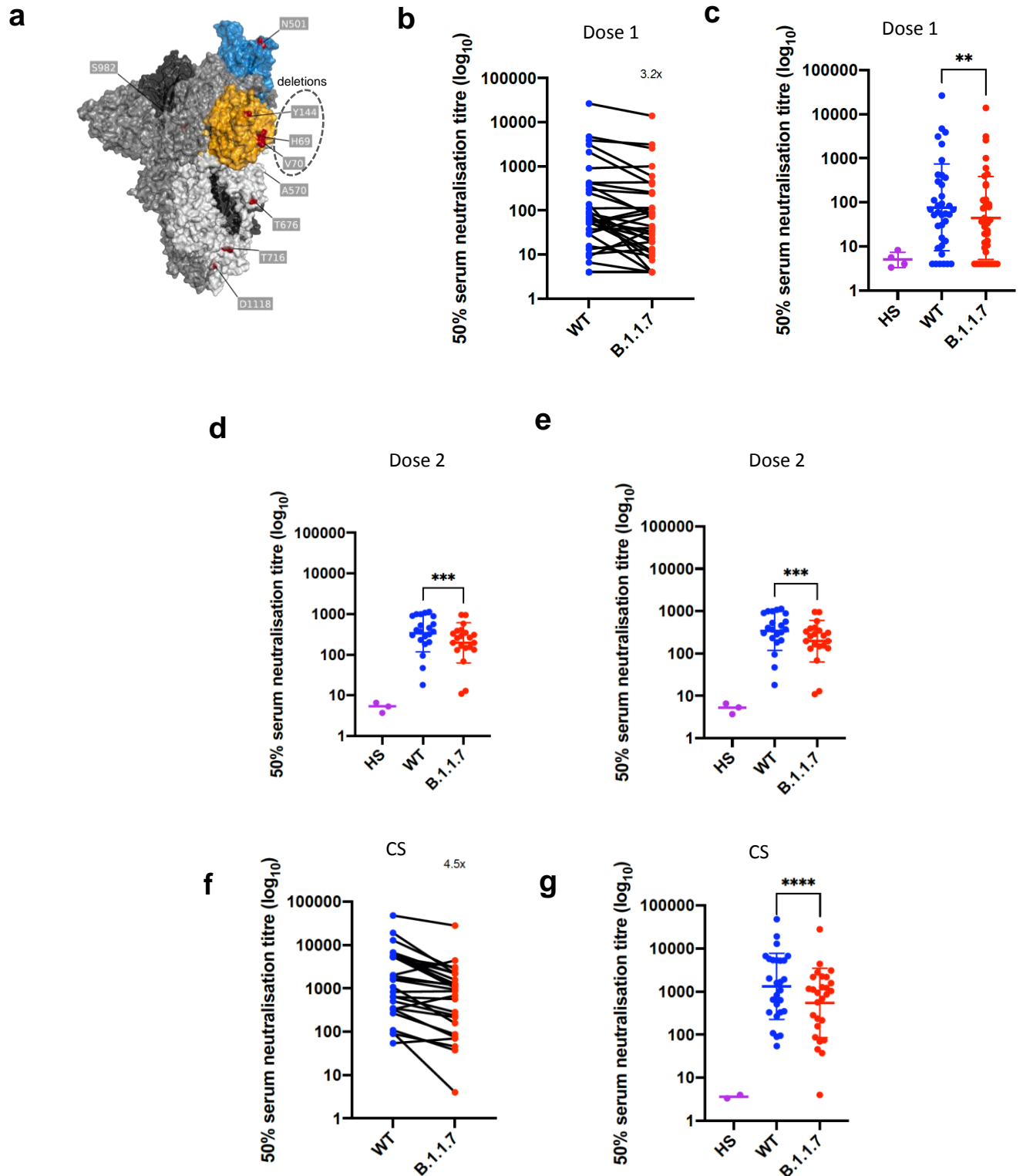


Figure 1. Neutralization by first and second dose mRNA vaccine sera against wild type and B.1.1.7 Spike mutant SARS-CoV-2 pseudotyped viruses. **a**, Spike in open conformation with a single erect RBD (PDB: 6ZGG) in trimer axis vertical view with the locations of mutated residues highlighted in red spheres and labelled on the monomer with erect RBD. Vaccine first dose (**b-c**, $n=37$), second dose (**d-e**, $n=21$) and convalescent sera, Conv. (**f-g**, $n=27$) against WT and B.1.1.7 Spike mutant with N501Y, A570D, Δ H69/V70, Δ 144/145, P681H, T716I, S982A and D1118H. GMT with s.d presented of two independent experiments each with two technical repeats. Wilcoxon matched-pairs signed rank test p-values * <0.05 , ** <0.01 , *** <0.001 , **** <0.0001 , ns not significant HS – human AB serum control. Limit of detection for 50% neutralization set at 10.

Figure 2

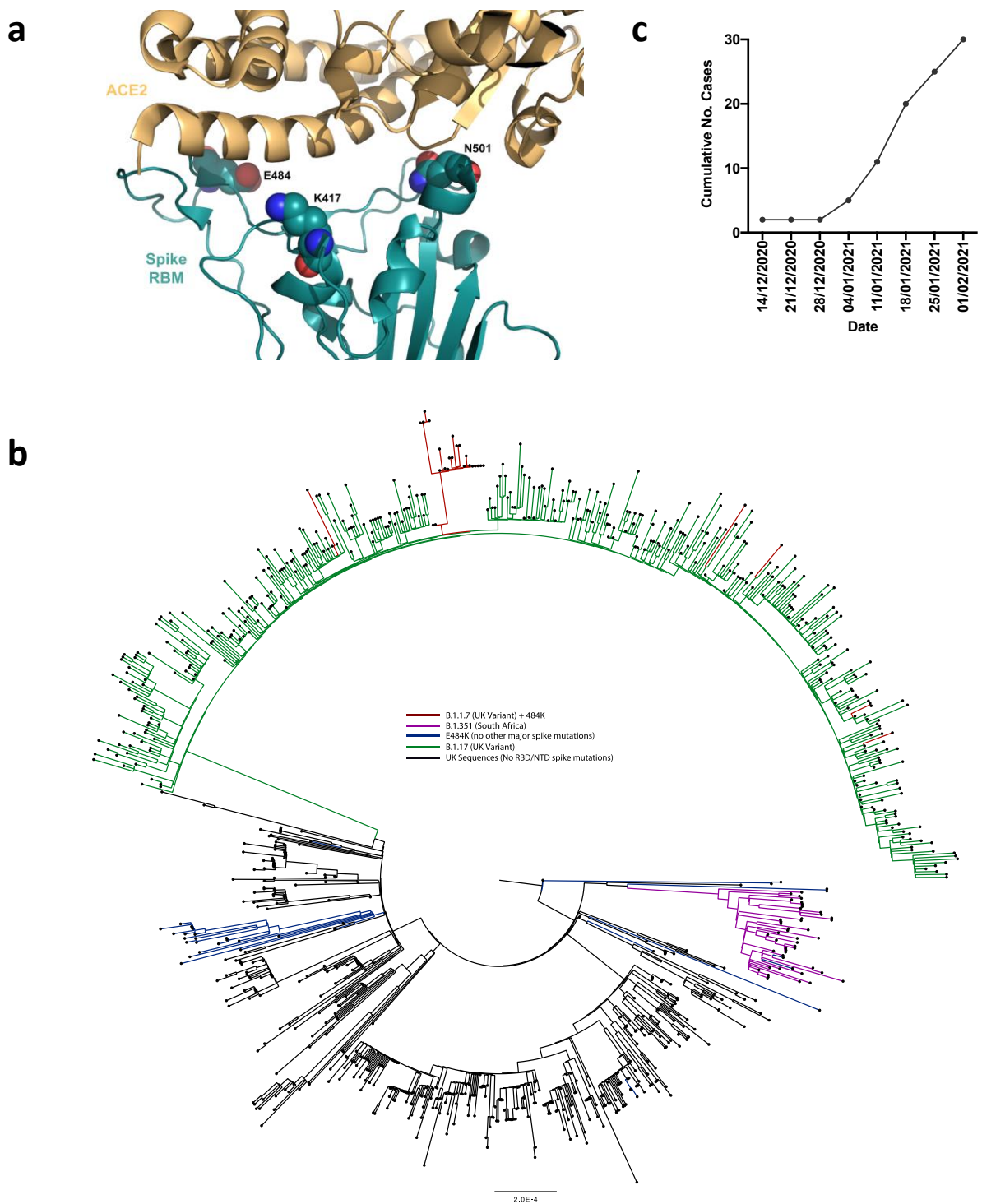


Figure 2. E484K appearing in background of B.1.1.7 with evidence of transmission a. Representation of Spike RBM:ACE2 interface (PDB: 6M0J) with residues E484, N501 and K417 highlighted as spheres coloured by element **b**. Maximum likelihood phylogeny of a subset of sequences from the United Kingdom bearing the E484K mutation (green) and lineage B.1.1.7 (blue), with background sequences without RBD mutations in black. As of 11th Feb 2021, 30 sequences from the B.1.1.7 lineage (one cluster of 25 at top of phylogenetic tree) have acquired the E484K mutation (red). **c.** Sequence accumulation over time in GISAID for UK sequences with B.1.1.7 and E484K. RBD – receptor binding domain; NTD – N terminal domain.

Figure 3

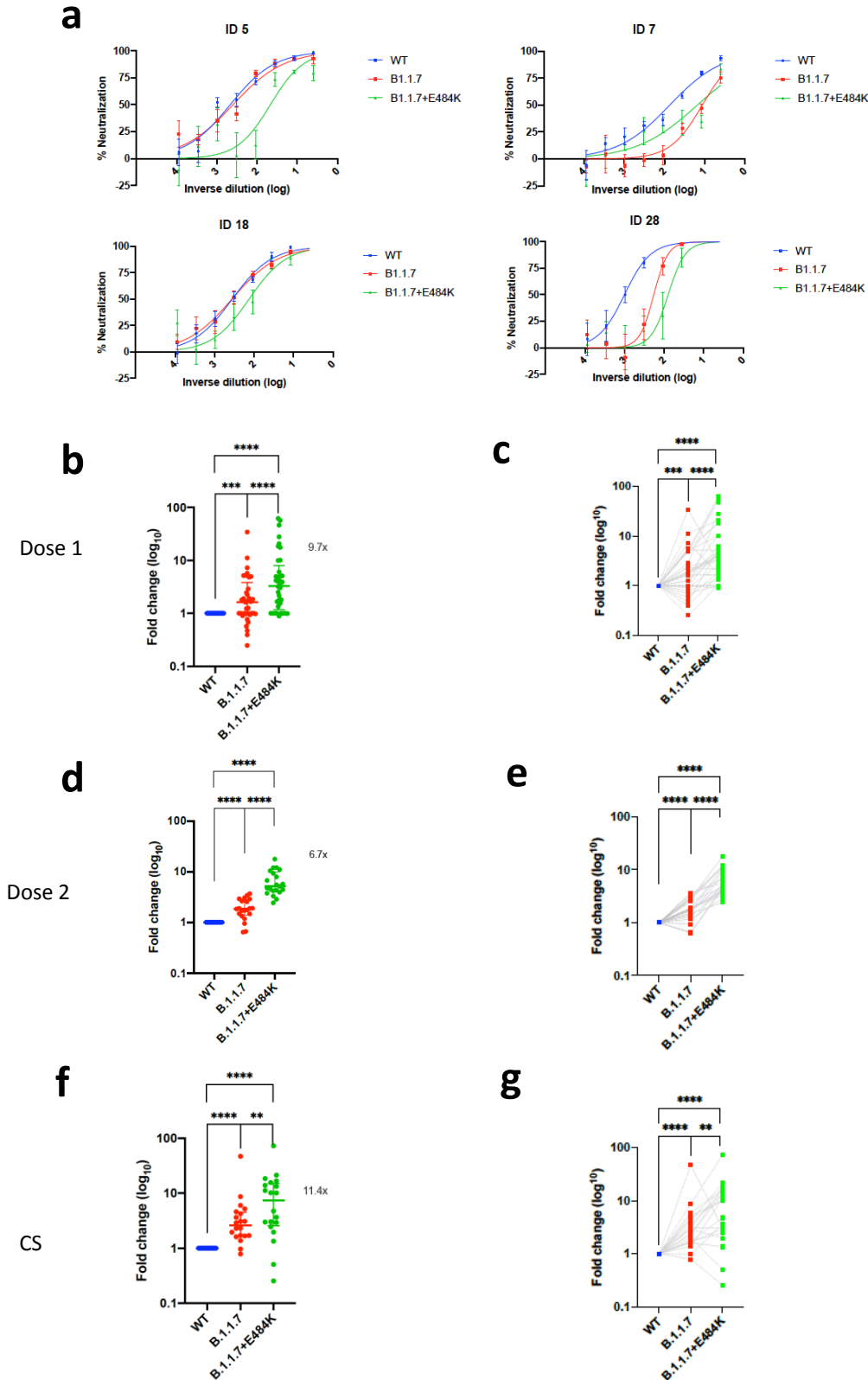
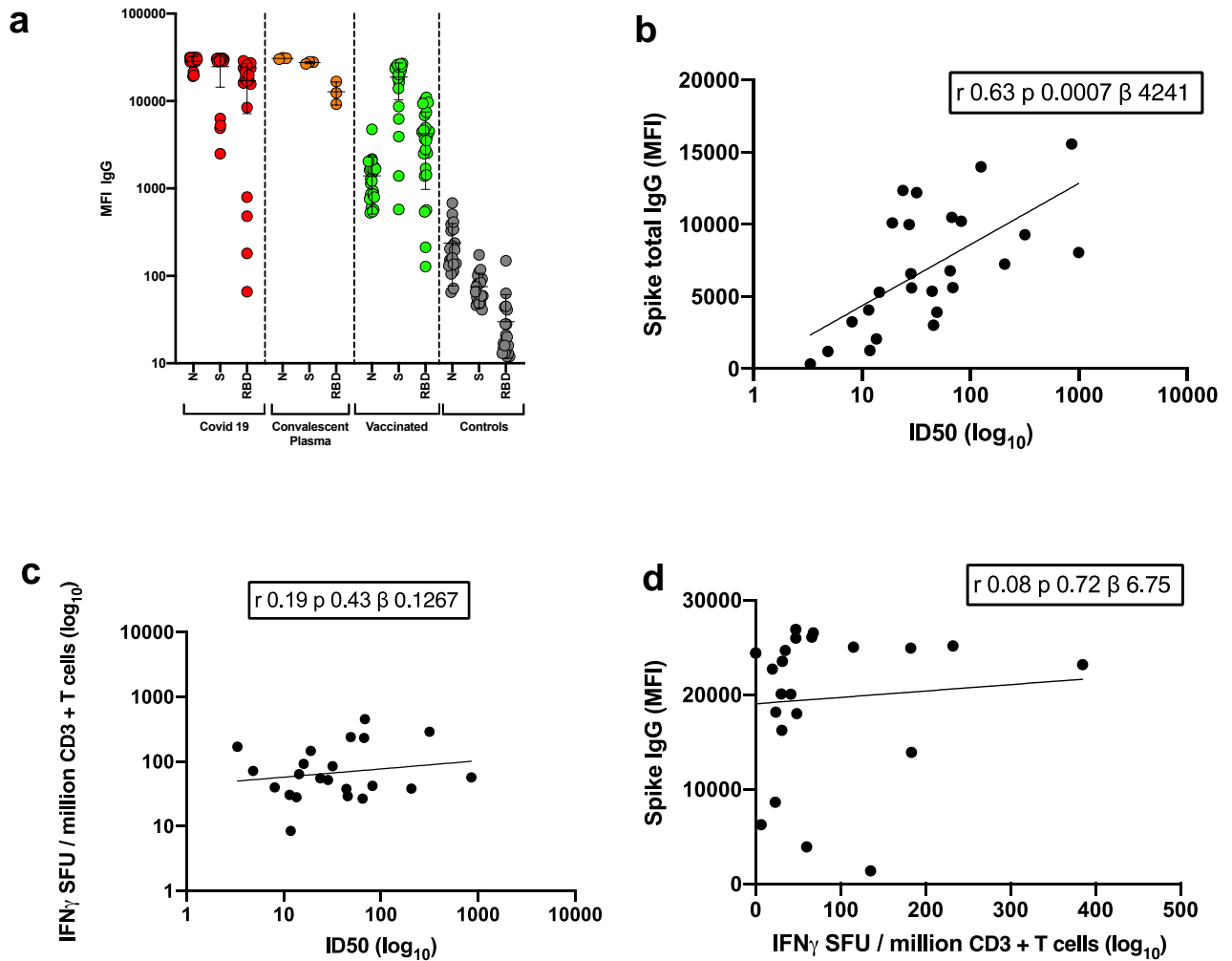


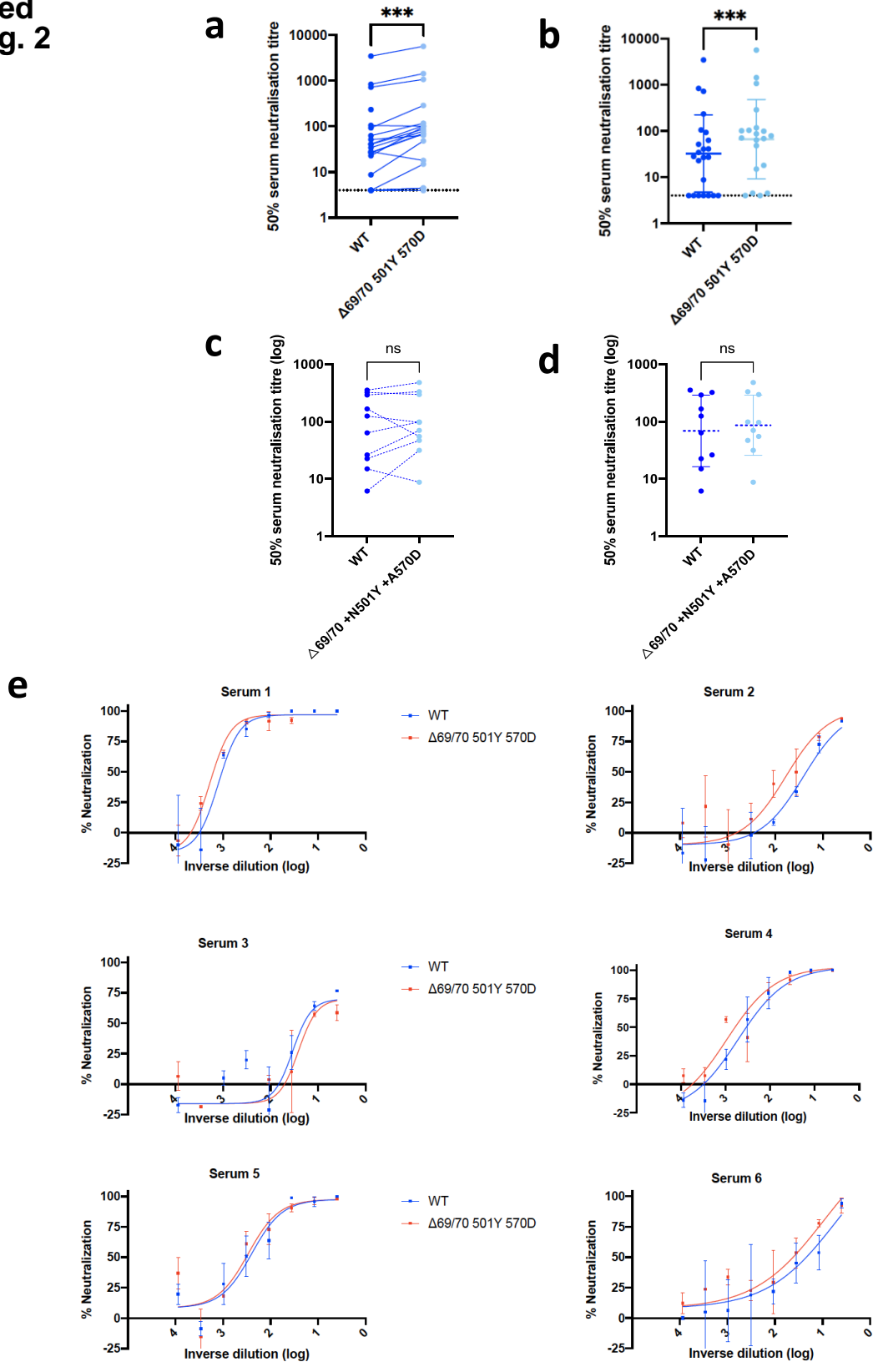
Figure 3. Neutralization potency of mRNA vaccine sera and convalescent sera (pre SARS-CoV-2 B.1.1.7) against pseudotyped virus bearing Spike mutations in the B.1.1.7 lineage with and without E484K in the receptor binding domain (all In Spike D614G background). a, Example neutralization curves for vaccinated individuals. Data points represent mean of technical replicates with standard error and are representative of two independent experiments (**b-g**). 50% neutralisation titre for each virus against sera derived (**b,c**, n=37) following first vaccination (**d,e**, n=21) following second vaccination and (**f,g**, n=20) convalescent sera (CS) expressed as fold change relative to WT. Data points are mean fold change of technical replicates and are representative of two independent experiments. Central bar represents mean with outer bars representing s.d. Wilcoxon matched-pairs signed rank test p-values * <0.05 , ** <0.01 , *** <0.001 , **** <0.0001 ; ns not significant. Limit of detection for 50% neutralization set at 10.

Extended Data Figure 1



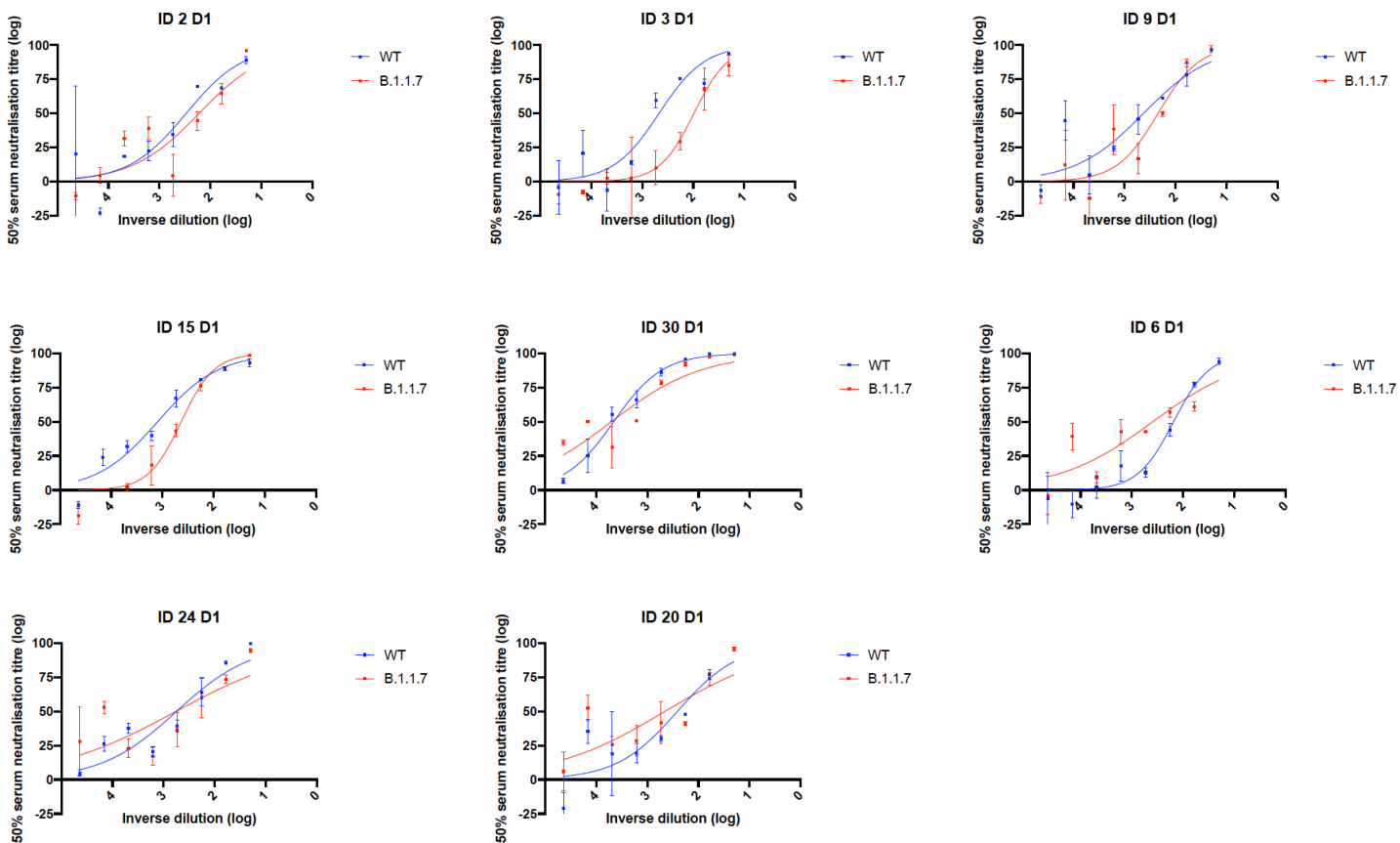
Extended Data Figure 1: Immune responses three weeks after first dose of Pfizer SARS-CoV-2 vaccine BNT162b2 **a**, Serum IgG responses against N protein, Spike and the Spike Receptor Binding Domain (RBD) from first vaccine participants (green), recovered COVID-19 cases (red), 3 convalescent plasma units and healthy controls (grey) as measured by a flow cytometry based Luminex assay. MFI, mean fluorescence intensity. Geometric mean titre (GMT with standard deviation (s.d) of two technical repeats presented. **b**, Relationship between serum IgG responses as measured by flow cytometry and serum neutralisation ID50. **c**, Relationship between serum neutralisation ID50 and T cell responses against SARS-CoV-2 by IFN gamma ELISpot. SFU: spot forming units. **d**, Relationship between serum IgG responses and T cell responses. Simple linear regression is presented with Pearson correlation (r), P-value (p) and regression coefficient/slope (β).

Extended Data Fig. 2



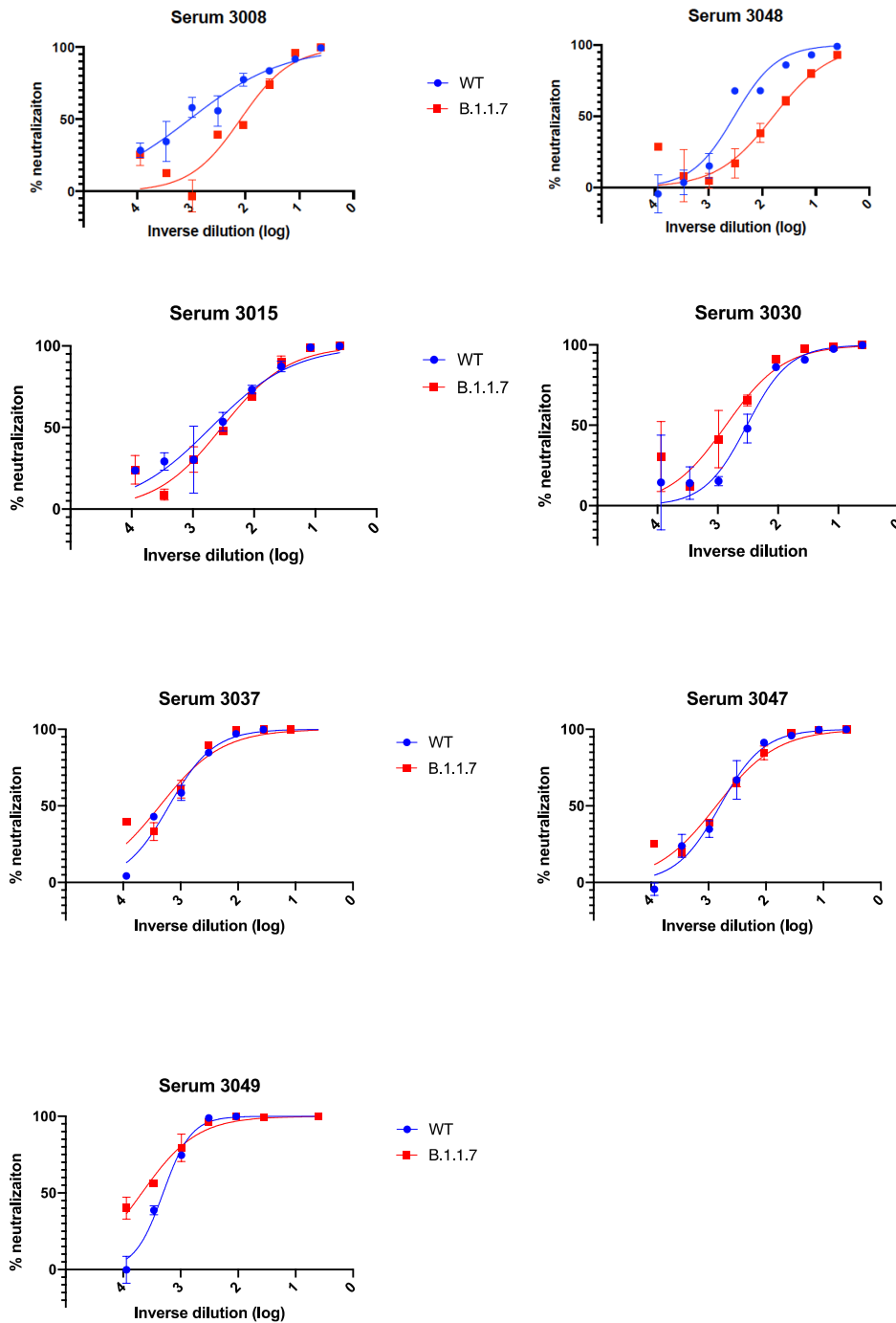
Extended data Fig 2. Neutralization by first dose BNT162b2 vaccine and convalescent sera against wild type and mutant (N501Y, A570D, Δ H69/V70) SARS-CoV-2 pseudotyped viruses: (a-b) Vaccine sera dilution for 50% neutralization against WT and Spike mutant with N501Y, A570D, Δ H69/V70. Geometric mean titre (GMT) + s.d of two independent experiments with two technical repeats presented. (c-d) Convalescent sera dilution for 50% neutralization against WT and Spike mutant with N501Y, A570D, Δ H69/V70. GMT + s.d of representative experiment with two technical repeats presented. **e**, Representative curves of convalescent serum log₁₀ inverse dilution against % neutralization for WT v N501Y, A570D, Δ H69/V70. Where a curve is shifted to the right this indicates the virus is less sensitive to the neutralizing antibodies in the serum. Data are means of technical replicates and error bars represent standard error of the mean. Data are representative of 2 independent experiments. Limit of detection for 50% neutralization set at 10.

Extended Data Fig. 3



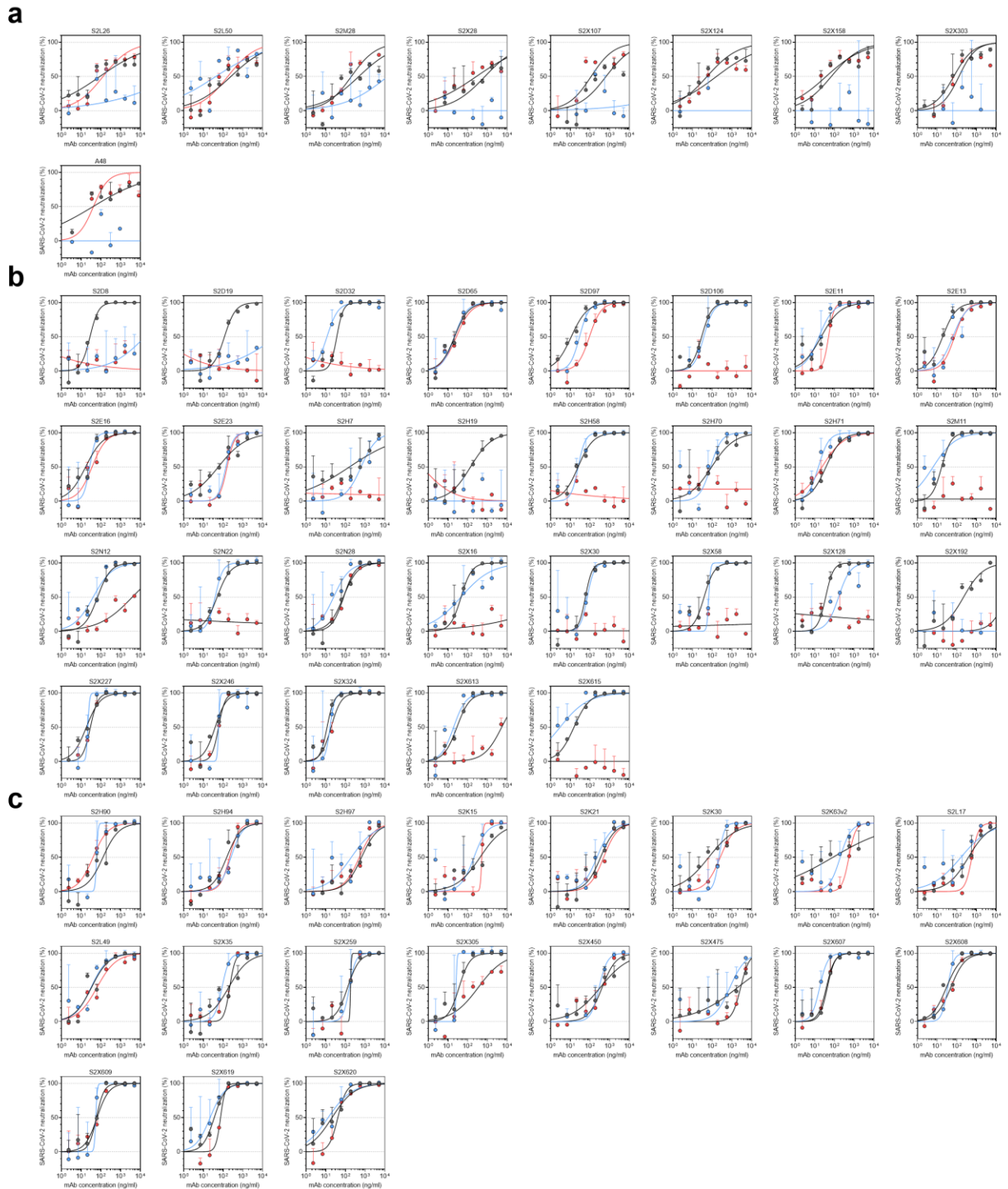
Extended Data Fig. 3. Representative neutralization curves of BNT162b2 vaccine sera against pseudovirus virus bearing eight Spike mutations present in B.1.1.7 versus wild type (all In Spike D614G background). Indicated is serum \log_{10} inverse dilution against % neutralization. Where a curve is shifted to the right this indicates the virus is less sensitive to the neutralizing antibodies in the serum. Data are for first dose of vaccine (D1). Data points represent means of technical replicates and error bars represent standard error of the mean. Limit of detection for 50% neutralization set at 10.

Extended Data Fig. 4



Extended Data Fig. 4. Representative neutralization curves of convalescent sera against wild type and B.1.1.7 Spike mutant SARS-CoV-2 pseudoviruses. Indicated is serum log₁₀ inverse dilution against % neutralization. Where a curve is shifted to the right this indicates the virus is less sensitive to the neutralizing antibodies in the serum. Data points represent means of technical replicates and error bars represent standard error of the mean. Limit of detection for 50% neutralization set at 10.

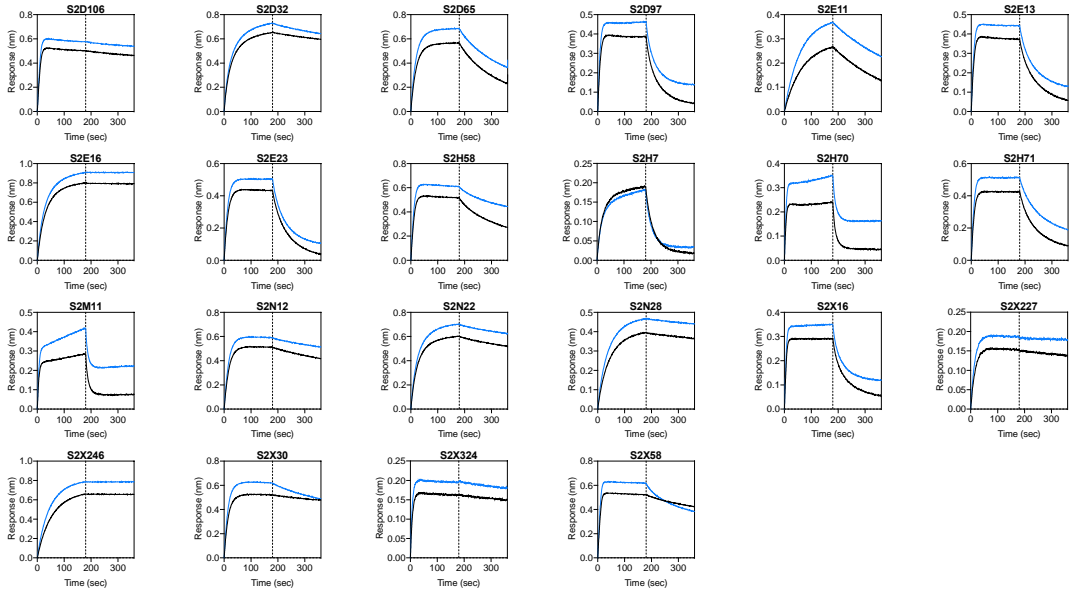
Extended Data Fig. 5



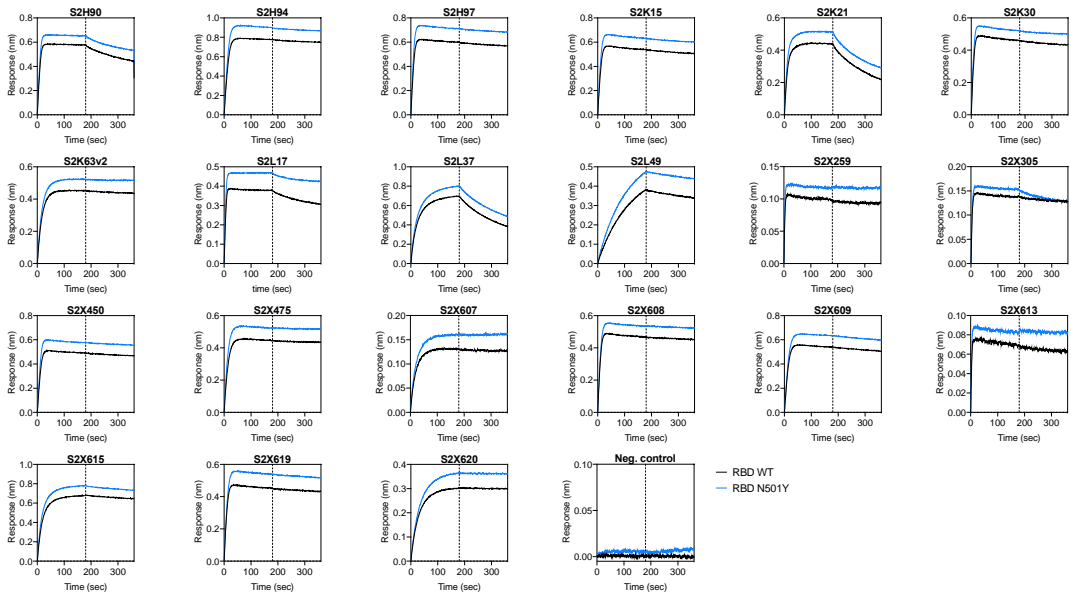
Extended Data Fig. 5. Neutralisation of WT (D614G), B.1.1.7 and TM (N501Y, E484K, K417N) SARS-CoV-2 Spike pseudotyped virus by a panel of 57 monoclonal antibodies (mAbs). **a-c**, Neutralisation of WT (black), B.1.1.7 (blue) and TM (red) SARS-CoV-2-MLV by 9 NTD-targeting (a), 29 RBM-targeting (b) and 19 non-RBM-targeting (c) mAbs.

Extended Data Fig. 6

a



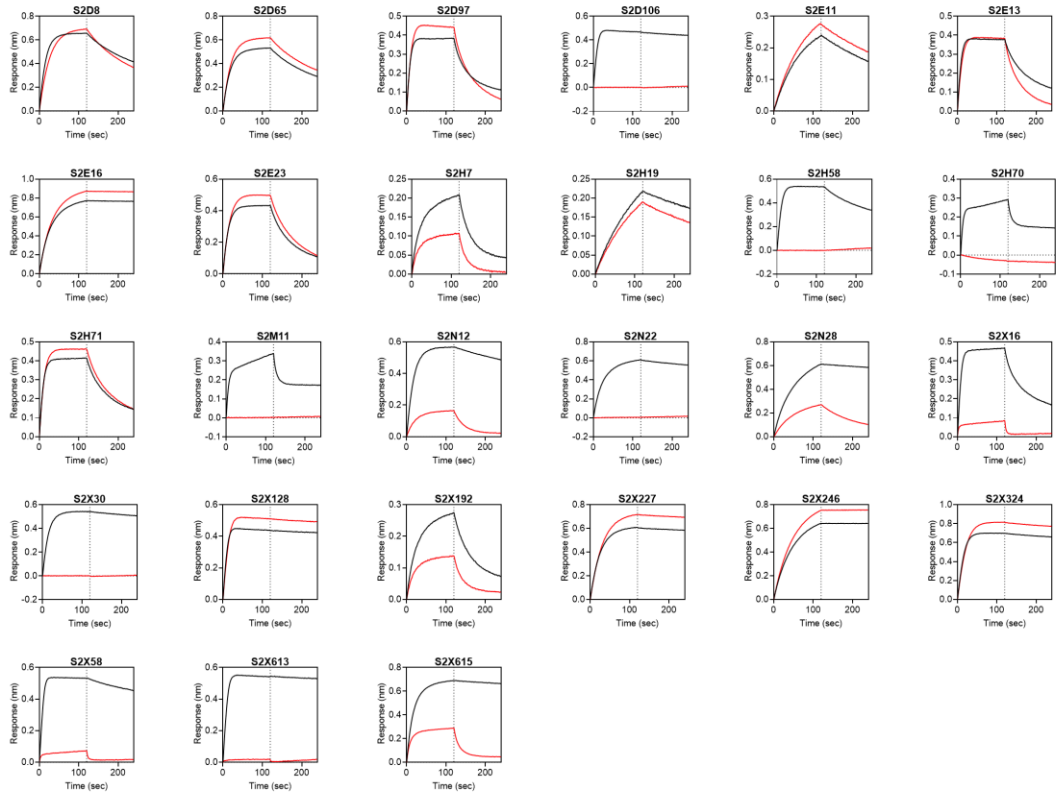
b



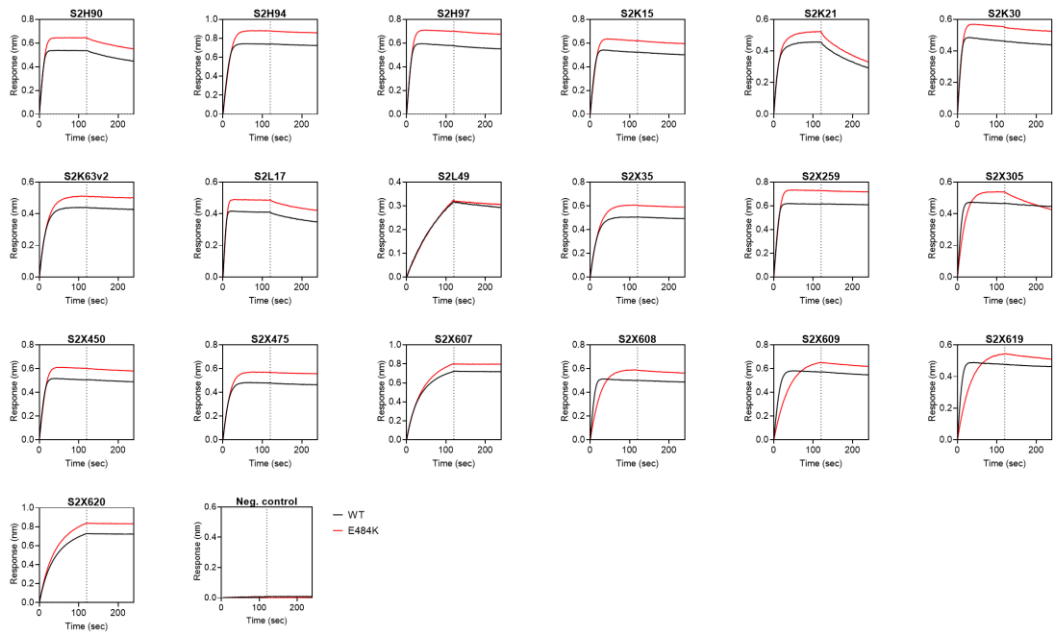
Extended Data Fig. 6. Kinetics of binding to WT and N501Y SARS-CoV-2 RBD of 43 RBD-specific mAbs. a-b, Binding to WT (black) and N501Y (blue) RBD by 22 RBM-targeting (a) and 21 non-RBM-targeting (b) mAbs. An antibody of irrelevant specificity was included as negative control. mAbs: monoclonal antibodies

Extended Data Fig. 7

a

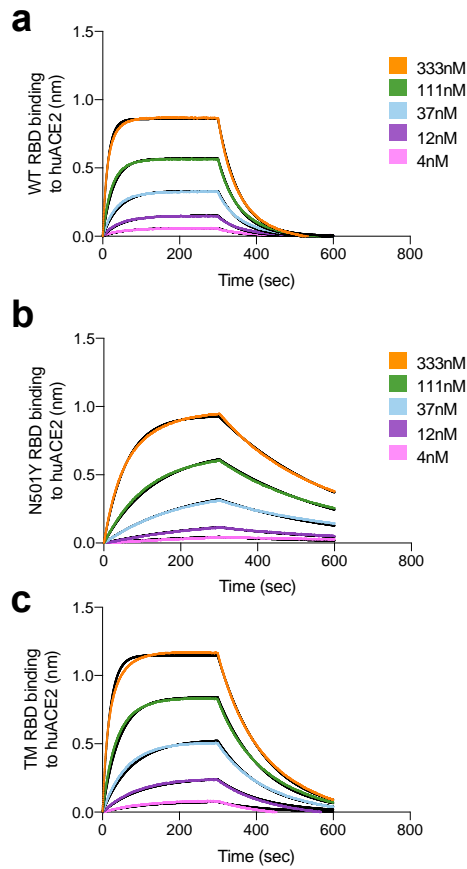


b



Extended Data Fig. 7. Kinetics of binding to WT and E484K SARS-CoV-2 RBD of 46 RBD-specific mAbs. a-b, Binding to WT (black) and E484K (red) RBD by 27 RBM-targeting (a) and 19 non-RBM-targeting (b) mAbs. An antibody of irrelevant specificity was included as negative control. mAbs: monoclonal antibodies

Extended Data Fig. 8



Extended Data Fig. 8. Binding of human ACE2 to SARS-CoV-2 WT, N501Y, TM (N501Y, E484K, K417N) RBDs. a-b. BLI binding analysis of the human ACE2 ectodomain (residues 1-615) to immobilized SARS-CoV-2 WT RBD (a) and B.1.1.7 RBD (b). Black lines correspond to a global fit of the data using a 1:1 binding model. RBD: receptor binding domain.